abnormalities result in severe neurodevelopmental delay and early onset epilepsy in both genders (Castren et al., 2011). In this study, the estimated frequencies of *CDKL5* abnormalities in patients with epileptic encephalopathy were 5% in male and 14% in female patients. Therefore, the observed difference in the frequency of *CDKL5* mutations between male and female patients may simply be a consequence of the fact that female patients have two X chromosomes.

Subjects in our study included five female patients with RTT who did not show *MECP2* mutations. However, these female patients did not carry a *CDKL5* mutation. Some researchers have found no *CDKL5* mutations in patients with RTT (Huppke et al., 2005; Li et al., 2007). Previously, *CDKL5* mutations were analyzed in patients with both classic and atypical variants of RTT. However, mutations were identified only in patients with seizure onset before 6 months of age (Evans et al., 2005; Scala et al., 2005; Artuso et al., 2010). In another study, all patients with *CDKL5* mutations showed early onset seizures that began before 6 months of age (Erez et al., 2009). These findings suggest that development of early onset seizures is an essential clinical feature in patients with *CDKL5* mutations. The onset of epileptic seizures in the first 6 months distinguishes patients with *CDKL5* mutations from patients with typical RTT caused by *MECP2* mutations (Castren et al., 2011).

All previously reported *CDKL5* mutations were sporadic and were identified as de novo. Only a small numbers of mutations were recurrent (Castren et al., 2011). In this study, we observed eight *CDKL5* mutations that included six novel and two recurrent mutations. The phenotypic features of the patients with recurrent mutations are similar to those described previously (Sartori et al., 2009; Artuso et al., 2010).

Consistent with the findings of previous studies, we observed polymorphous seizures (i.e., myoclonic seizures, tonic seizures, and spasms) in our study. The clinical course of seizure development was also identical to the proposed three stages reported by Bahi-Buisson et al. (2008a) [i.e., stage I, early onset epilepsy (onset 1–10 weeks); stage II, epileptic encephalopathy with infantile spasms and hypsarrhythmia; stage III, seizure-free in estimated 50% of patients at late infantile period] because our Patient 7 showed good seizure control after 3 years of age. Artuso et al. (2010) reported that patients with *CDKL5* mutations showed no abnormalities on brain magnetic resonance imaging (MRI). However, our findings indicated mild frontal lobe atrophy in almost all patients. Therefore, this may be an additional clinical characteristic of patients with *CDKL5* mutations.

## Acknowledgments

We thank the patients' parents for their gracious participation and support. J-S L was supported by a Research Fellowship from the Takeda Science Foundation in Japan. This research was partially supported by Research Grant from the Japan Epilepsy Research Foundation (T.Y.)

## Disclosure

None of the authors has any conflict of interest to disclose. We confirm that we have read the Journal's position on issues involved in ethical publication and affirm that this report is consistent with those guidelines.

## References

Archer HL, Evans J, Edwards S, Colley J, Newbury-Ecob R, O'Callaghan F, Huyton M, O'Regan M, Tolmie J, Sampson J, Clarke A, Osborne J. (2006) CDKL5 mutations cause infantile spasms, early onset seizures, and severe mental retardation in female patients. *J Med Genet* 43:729–734.

Artuso R, Mencarelli MA, Polli R, Sartori S, Ariani F, Pollazzon M, Marozza A, Cilio MR, Specchio N, Vigevano F, Vecchi M, Boniver C, Bernardina BD, Parmeggiani A, Buoni S, Hayek G, Mari F, Renieri A, Murgia A. (2010) Early-onset seizure variant of Rett syndrome: definition of the clinical diagnostic criteria. *Brain Dev* 32:17–24.

Bahi-Buisson N, Kaminska A, Boddaert N, Rio M, Afenjar A, Gerard M, Giuliano F, Motte J, Heron D, Morel MA, Plouin P, Richelme C, des Portes V, Dulac O, Philippe C, Chiron C, Nabbout R, Bienvenu T. (2008a) The three stages of epilepsy in patients with CDKL5 mutations. *Epilepsia* 49:1027–1037.

Bahi-Buisson N, Nectoux J, Rosas-Vargas H, Milh M, Boddaert N, Girard B, Cances C, Ville D, Afenjar A, Rio M, Heron D, N'Guyen Morel MA, Arzimanoglou A, Philippe C, Jonveaux P, Chelly J, Bienvenu T. (2008b) Key clinical features to identify girls with CDKL5 mutations. *Brain* 131:2647–2661.

Bahi-Buisson N, Girard B, Gautier A, Nectoux J, Fichou Y, Saillour Y, Poirier K, Chelly J, Bienvenu T. (2010) Epileptic encephalopathy in a girl with an interstitial deletion of Xp22 comprising promoter and exon 1 of the CDKL5 gene. *Am J Med Genet B Neuropsychiatr Genet* 153B:202–207.

Castren M, Gaily E, Tengstrom C, Lahdetie J, Archer H, Ala-Mello S. (2011) Epilepsy caused by CDKL5 mutations. *Eur J Paediatr Neurol* 15:65–69.

Elia M, Falco M, Ferri R, Spalletta A, Bottitta M, Calabrese G, Carotenuto M, Musumeci SA, Lo Giudice M, Fichera M. (2008) CDKL5 mutations in boys with severe encephalopathy and early-onset intractable epilepsy. *Neurology* 71:997–999.

Erez A, Patel AJ, Wang X, Xia Z, Bhatt SS, Craigen W, Cheung SW, Lewis RA, Fang P, Davenport SL, Stankiewicz P, Lalani SR. (2009) Alu-specific microhomology-mediated deletions in CDKL5 in females with early-onset seizure disorder. *Neurogenetics* 10:363–369.

Evans JC, Archer HL, Colley JP, Ravn K, Nielsen JB, Kerr A, Williams E, Christodoulou J, Gecz J, Jardine PE, Wright MJ, Pilz DT, Lazarou L, Cooper DN, Sampson JR, Butler R, Whatley SD, Clarke AJ. (2005) Early onset seizures and Rett-like features associated with mutations in CDKL5. *Eur J Hum Genet* 13:1113–1120.

Fichou Y, Bieth E, Bahi-Buisson N, Nectoux J, Girard B, Chelly J, Chaix Y, Bienvenu T. (2009) Re: CDKL5 mutations in boys with severe encephalopathy and early-onset intractable epilepsy. *Neurology* 73:77–78; author reply 78.

Fichou Y, Nectoux J, Bahi-Buisson N, Chelly J, Bienvenu T. (2010) An isoform of the severe encephalopathy-related CDKL5 gene, including a novel exon with extremely high sequence conservation, is specifically expressed in brain. *J Hum Genet* 56:52–57.

Gomot M, Gendrot C, Verloes A, Raynaud M, David A, Yntema HG, Dessay S, Kalscheuer V, Frints S, Couvert P, Briault S, Blesson S, Toutain A, Chelly J, Desportes V, Moraine C. (2003) MECP2 gene mutations in non-syndromic X-linked mental retardation: phenotype-genotype correlation. *Am J Med Genet A* 123A:129–139.

Huppke P, Ohlenbusch A, Brendel C, Laccone F, Gartner J. (2005) Mutation analysis of the HDAC 1, 2, 8 and CDKL5 genes in Rett syndrome patients without mutations in MECP2. *Am J Med Genet A* 137: 136–138.

Kalscheuer VM, Tao J, Donnelly A, Hollway G, Schwinger E, Kubart S, Menzel C, Hoeltzenbein M, Tommerup N, Eyre H, Harbord M, Haan E, Sutherland GR, Ropers HH, Gecz J. (2003) Disruption of the serine/threonine kinase 9 gene causes severe X-linked infantile spasms and mental retardation. *Am J Hum Genet* 72:1401–1411.

Li MR, Pan H, Bao XH, Zhang YZ, Wu XR. (2007) MECP2 and CDKL5 gene mutation analysis in Chinese patients with Rett syndrome. *J Hum Genet* 52:38–47.

Mari F, Azimonti S, Bertani I, Bolognese F, Colombo E, Caselli R, Scala E, Longo I, Grosso S, Pescucci C, Ariani F, Hayek G, Balestri P, Bergo A, Badaracco G, Zappella M, Broccoli V, Renieri A, Kilstrup-Nielsen C, Landsberger N. (2005) CDKL5 belongs to the same molecular pathway of MeCP2 and it is responsible for the early-onset seizure variant of Rett syndrome. *Hum Mol Genet* 14:1935–1946.

Mei D, Marini C, Novara F, Bernardina BD, Granata T, Fontana E, Parrini E, Ferrari AR, Murgia A, Zuffardi O, Guerrini R. (2010) Xp22.3 genomic deletions involving the CDKL5 gene in girls with early onset epileptic encephalopathy. *Epilepsia* 51:647–654.

Nabbout R, Dulac O. (2003) Epileptic encephalopathies: a brief overview. *J Clin Neurophysiol* 20:393–397.

Nabbout R, Dulac O. (2008) Epileptic syndromes in infancy and childhood. *Curr Opin Neurol* 21:161–166.

Nemos C, Lambert L, Giuliano F, Doray B, Roubertie A, Goldenberg A, Delobel B, Layet V, N'Guyen MA, Saunier A, Verneau F, Jonveaux P, Philippe C. (2009) Mutational spectrum of CDKL5 in early-onset encephalopathies: a study of a large collection of French patients and review of the literature. *Clin Genet* 76:357–371.

Pintaudi M, Baglietto MG, Gaggero R, Parodi E, Pessagno A, Marchi M, Russo S, Veneselli E. (2008) Clinical and electroencephalographic features in patients with CDKL5 mutations: two new Italian cases and review of the literature. *Epilepsy Behav* 12:326–331.

Sartori S, Di Rosa G, Polli R, Bettella E, Tricomi G, Tortorella G, Murgia A. (2009) A novel CDKL5 mutation in a 47,XXY boy with the early-onset seizure variant of Rett syndrome. *Am J Med Genet A* 149A:232–236.

Scala E, Ariani F, Mari F, Caselli R, Pescucci C, Longo I, Meloni I, Giachino D, Bruttini M, Hayek G, Zappella M, Renieri A. (2005) CDKL5/STK9 is mutated in Rett syndrome variant with infantile spasms. *J Med Genet* 42:103–107.

Shimojima K, Sugiura C, Takahashi H, Ikegami M, Takahashi Y, Ohno K, Matsuo M, Saito K, Yamamoto T. (2010) Genomic copy number variations at 17p13.3 and epileptogenesis. *Epilepsy Res* 89:303–309.

Van Esch H, Jansen A, Bauters M, Froyen G, Fryns JP. (2007) Encephalopathy and bilateral cataract in a boy with an interstitial deletion of Xp22 comprising the CDKL5 and NHS genes. *Am J Med Genet A* 143:364–369.

Zupanc ML. (2009) Clinical evaluation and diagnosis of severe epilepsy syndromes of early childhood. *J Child Neurol* 24:6S–14S.

## Supporting Information

Additional Supporting Information may be found in the online version of this article:

**Table S1.** The physical positions of BAC clones.

**Table S2.** Primer sequences for *CDKL5*.

**Table S3.** The results of aCGH.

Please note: Wiley-Blackwell is not responsible for the content or functionality of any supporting information supplied by the authors. Any queries (other than missing material) should be directed to the corresponding author for the article.

RESEARCH ARTICLE

AMERICAN JOURNAL OF medical genetics

# *MBTPS2* Mutation Causes BRESEK/BRESHECK Syndrome

**Misako Naiki,[1,2] Seiji Mizuno,[3] Kenichiro Yamada,[1] Yasukazu Yamada,[1] Reiko Kimura,[1] Makoto Oshiro,[4] Nobuhiko Okamoto,[5] Yoshio Makita,[6] Mariko Seishima,[7] and Nobuaki Wakamatsu[1]***

[1]Department of Genetics, Institute for Developmental Research, Aichi Human Service Center, Kasugai, Aichi, Japan

[2]Department of Pediatrics, Nagoya University Graduate School of Medicine, Nagoya, Aichi, Japan

[3]Department of Pediatrics, Central Hospital, Aichi Human Service Center, Kasugai, Aichi, Japan

[4]Department of Pediatrics, Japanese Red Cross Nagoya Daiichi Hospital, Nagoya, Aichi, Japan

[5]Department of Medical Genetics, Osaka Medical Center and Research Institute for Maternal and Child Health, Izumi, Osaka, Japan

[6]Education Center, Asahikawa Medical University, Asahikawa, Hokkaido, Japan

[7]Department of Dermatology, Gifu University Graduate School of Medicine, Gifu, Gifu, Japan

Received 25 July 2011; Accepted 17 October 2011

BRESEK/BRESHECK syndrome is a multiple congenital malformation characterized by brain anomalies, intellectual disability, ectodermal dysplasia, skeletal deformities, ear or eye anomalies, and renal anomalies or small kidneys, with or without Hirschsprung disease and cleft palate or cryptorchidism. This syndrome has only been reported in three male patients. Here, we report on the fourth male patient presenting with brain anomaly, intellectual disability, growth retardation, ectodermal dysplasia, vertebral (skeletal) anomaly, Hirschsprung disease, low-set and large ears, cryptorchidism, and small kidneys. These manifestations fulfill the clinical diagnostic criteria of BRESHECK syndrome. Since all patients with BRESEK/BRESHECK syndrome are male, and X-linked syndrome of ichthyosis follicularis with atrichia and photophobia is sometimes associated with several features of BRESEK/BRESHECK syndrome such as intellectual disability, vertebral and renal anomalies, and Hirschsprung disease, we analyzed the causal gene of ichthyosis follicularis with atrichia and photophobia syndrome, *MBTPS2*, in the present patient and identified an p.Arg429His mutation. This mutation has been reported to cause the most severe type of ichthyosis follicularis with atrichia and photophobia syndrome, including neonatal and infantile death. These results demonstrate that the p.Arg429His mutation in *MBTPS2* causes BRESEK/BRESHECK syndrome. 

**Key words:** BRESEK/BRESHECK syndrome; IFAP syndrome; *MBTPS2*; mutation; S2P

How to Cite this Article:
Naiki M, Mizuno S, Yamada K, Yamada Y, Kimura R, Oshiro M, Okamoto N, Makita Y, Seishima M, Wakamatsu N. 2011. *MBTPS2* mutation causes BRESEK/BRESHECK syndrome.
Am J Med Genet Part A .

## INTRODUCTION

BRESEK/BRESHECK syndrome (OMIM# 300404), a multiple congenital malformation disorder characterized by brain anomalies, intellectual disability, ectodermal dysplasia, skeletal deformities, Hirschsprung disease, ear or eye anomalies, cleft palate or cryptorchidism, and kidney dysplasia/hypoplasia [Reish et al., 1997]. The acronym BRESEK refers to the common findings, whereas BRESHECK refers to all manifestations. Because the first two patients were maternally related half brothers, an X-linked disorder was proposed. Although each symptom of these patients is often observed in other congenital diseases, the combination of all symptoms is rare, and only one additional patient with BRESEK has been reported to date [Tumialán and Mapstone, 2006]. Here, we present the fourth male patient with multiple anomalies. The patient presented with a variety of clinical features that were consistent with those of the previously reported BRESHECK syndrome.

The syndrome of ichthyosis follicularis with atrichia and photophobia (IFAP, OMIM# 308205), an X-linked recessive oculocutaneous disorder, is characterized by a peculiar triad of ichthyosis follicularis, total or subtotal atrichia, and varying degrees

Grant sponsor: Takeda Science Foundation; Grant sponsor: Health Labour Sciences Research Grant.
*Correspondence to:
Nobuaki Wakamatsu, Department of Genetics, Institute for Developmental Research, Aichi Human Service Center, 713-8 Kamiya-cho, Kasugai, Aichi 480-0392, Japan. E-mail: nwaka@inst-hsc.jp
Published online 00 Month 2011 in Wiley Online Library (wileyonlinelibrary.com).
DOI 10.1002/ajmg.a.34373

of photophobia [MacLeod, 1909]. Martino et al. [1992] reported a male patient with IFAP syndrome presented with short stature, intellectual disability, seizures, hypohidrosis, enamel dysplasia, congenital aganglionic megacolon, inguinal hernia, vertebral and renal anomalies, and the classic symptom triad of IFAP syndrome. This report broadened the clinical features of IFAP syndrome. It should be noted that the clinical symptoms of this patient are quite similar to those of BRESHECK syndrome, with the exception of cleft palate, cryptorchidism, and photophobia (Patient 5; Table I). The gene mutated in patients with IFAP syndrome, *MBTPS2* (GenBank reference sequence NM_015884), was identified from a variety of clinical features of IFAP syndrome, including the triad and neonatal death [Oeffner et al., 2009]. Thus, the mode of inheritance and several clinical features are common to both BRESEK/BRESHECK and IFAP syndromes. These findings prompted us to perform mutation analysis of *MBTPS2* in the present patient, resulting in the identification of a missense mutation.

## MATERIALS AND METHODS

### Patients

Written informed consent was obtained from the parents of the patient. Experiments were conducted after approval of the institutional review board of the Institute for Developmental Research, Aichi Human Service Center. The patient (II-1; Fig. 3) was born to a 31-year-old mother (I-2) and a 31-year-old father (I-1), both healthy Japanese individuals without consanguinity. His mother miscarried her first child at 5 weeks. The pregnancy of the patient reported here was complicated with mild oligohydramnios, and he was delivered by caesarean because of a breech position at 38 weeks of gestation. His birth weight was 1,996 g (−2.6 SD), and he measured 44 cm (−2.6 SD) in length with an occipitofrontal circumference of 32.5 cm (−0.5 SD). Apgar scores at 1 and 5 min were four and eight, respectively. The patient exhibited generalized alopecia and lacked eyelashes, scalp hair, and eyebrows (Fig. 1A). The skin on the entire body was erythematous with

TABLE I. Clinical Features of BRESEK/BRESHECK and IFAP Syndromes and *MBTPS2* Mutation

| | BRESEK/BRESHECK syndrome | | | | IFAP syndrome | | |
|---|---|---|---|---|---|---|---|
| **Patient** | **1** | **2** | **3** | **4** | **5** | **6** | **7** |
| Clinical features | | | | | | | |
| Gender | M | M | M | M | M | M | M |
| Gestational age (weeks) | 32 | 40 | ND | 38 | 30 | ND | ND |
| Birth weight (g) | 990 | 2,230 | ND | 1,996 | 2,040 | ND | ND |
| Intrauterine growth retardation | + | + | ND | + | − | ND | ND |
| Major features | | | | | | | |
| Follicular ichthyosis | − | − | ND | − | + | + | + |
| Atrichia | + | + | + | + | + | + | + |
| Photophobia | − | − | − | + | + | + | + |
| Brain malformation | + | + | + | + | + | − | + |
| Mental and growth retardation | + | + | + | + | + | + | + |
| Skeletal (Vertebrate) anomalies | + | + | + | + | + | + | + |
| Hirschsprung disease | − | + | + | + | + | + | + |
| Eye malformation or | + | + | + | − | + | − | − |
| Large ears | + | + | + | + | + | − | − |
| Cleft lip/palate or | − | + | − | − | − | + | − |
| Cryptorchidism | + | + | − | + | − | − | − |
| Kidney malformation | + | + | − | + | + | + | + |
| Other features | | | | | | | |
| Microcephaly | + | + | + | + | + | − | + |
| Seizures | − | + | + | + | + | − | + |
| Deafness | − | + | − | + | − | − | − |
| Hand anomalies | + | + | + | − | + | + | + |
| Cardiac anomalies | − | − | + | − | − | − | + |
| Inguinal hernia | − | − | − | − | + | + | + |
| Trachea anomalies | − | − | − | + | − | − | − |
| Regression | − | − | − | + | − | − | − |
| Age | 6 h d | 7 y | 1.5 y | 8 y | 3 y | 9 m d | 14 m d |
| *MBTPS2* mutation | NP | NP | NP | R429H | NP | R429H | R429H |

+, present;−, not present; M, male; ND, not described; NP, not performed; h, hour; d, dead; m, month; y, year; R429H, Arg429His; BRESEK/BRESHECK syndrome, (Patients 1-4); IFAP syndrome, (Patients 5–7); Patients: 1, Reish et al. [1997] patient 1; 2, Reish et al. [1997] patient 2; 3, Tumialán and Mapstone [2006]; 4, present case; 5, Martino et al. [1992]; 6, Oeffner et al. [2009] 3-III:3; 7, Oeffner et al. [2009] 3-III:4.

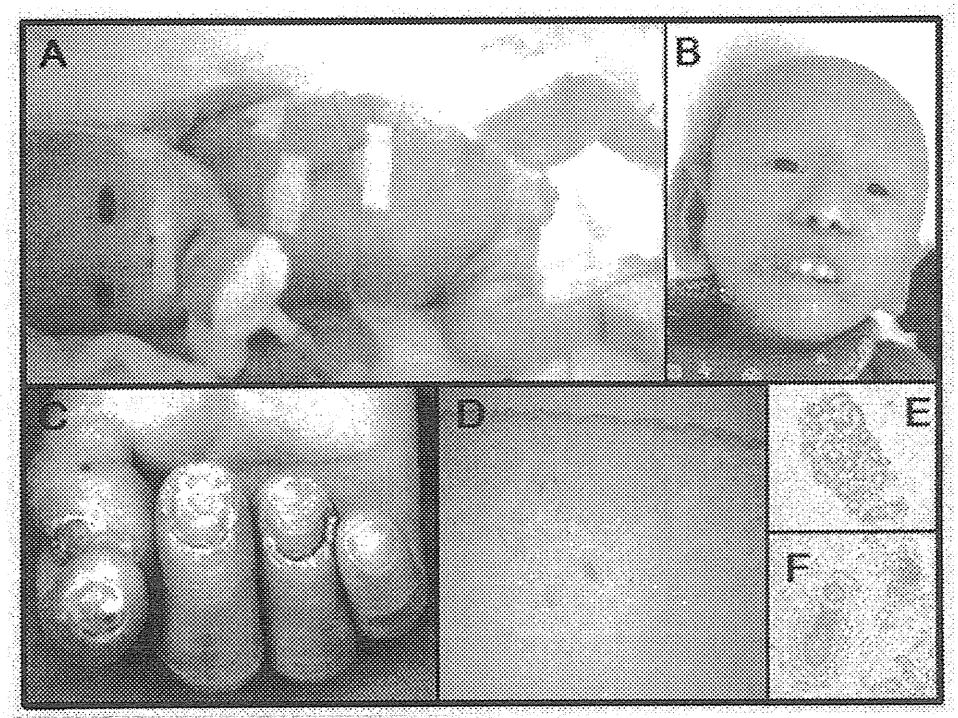


**FIG. 1. Clinical appearance and dermatological findings of the patient. A: Lateral view of the patient at birth. Note the generalized alopecia with an absence of scalp hair, eyebrows, and eyelashes. The skin was dry and scaly, and an itchy erythema was observed over the entire body. B: Frontal view of the patient at 4 years of age. Note the characteristic facial appearance with long, malformed ears, a relatively high nasal bridge, and a wide nasal base. C: The patient had normal-sized but deformed and thickened nails. D–F: Histologic examination of the abdominal skin at the age of 15 months showed a reduced number of hair follicles (D), normal eccrine glands (E), and hypoplastic hair follicles (F).**

continuous desquamation (Fig. 1A). He had malformed large ears, an inferiorly curved penis, and a bifid scrotum. The testicles were not palpable. He experienced persistent constipation, and total colonic Hirschsprung disease was confirmed through barium enema (Fig. 2E) and rectal biopsy at 2 months. A bone survey performed using three-dimensional (3D) computed tomography (CT) showed abnormal imbalanced hemivertebrae in the two lowest thoracic vertebral bodies (Fig. 2C). The patient's right kidney was smaller than normal. Brain magnetic resonance imaging (MRI) at 3 years of age demonstrated decreased volumes of the frontal and parietal lobes and thinning of the corpus callosum with dilatation of the ventricles (Fig. 2A,B). There were no abnormalities of the eyes or optic nerves. We concluded that the patient had BRESHECK syndrome. The patient had seizures at 5 months of age with an apneic episode and cyanosis. Electroencephalographic (EEG) analysis showed abnormal patterns of sharp waves in the posterior lobe. The seizures were almost completely controlled with phenobarbital. The patient was allergic to milk. At 7 months, tracheal endoscopy revealed subglottic tracheal stenosis and abnormal segmentation of the left lung. A chest CT performed at 3 years of age showed a congenital cystic adenomatoid malformation (CCAM) in the right upper lobe (Fig. 2D). Auditory brain stem responses showed bilateral 80 dB hearing loss at 8 months of age.

The patient exhibited delayed psychomotor development during his infancy. He could drink from a bottle at the age of 3 months and could sit up unsupported at 15 months. Abdominal skin biopsy at 15 months revealed reduced number of hair follicles (Fig. 1D). The eccrine glands were normal (Fig. 1E), and most of his hair follicles appeared to be hypoplastic (Fig. 1F). These findings were similar to ichthyosiform erythroderma. Photophobia was noted when the patient left the hospital and first went outside at 18 months of age. At 2 years and 6 months of age, he had a series of epileptic episodes. He experienced a maximum of 100 seizures per day, and EEG analysis showed continual abnormal spikes in the posterior lobe. The seizures were controlled with clonazepam therapy. At 2 years and 9 months of age, he could stand with support and displayed social smiles when interacting with other people. However, the patient developed psychomotor regression at the age of 3 years. He exhibited a progressive loss of emotional response to others, developed hypotonia, and could not stand or sit alone. At 4 years of age, he became bedridden and showed almost no response to people. He had highly desquamated skin, similar to that seen in ichthyosis (Fig. 1B), and easily developed erythema on the skin of the entire body. The patient had deformed and thickened nails (Fig. 1C). He had persistent corneal erosions, but ophthalmoscopy could not be performed at the age of 4 years because of corneal opacification.

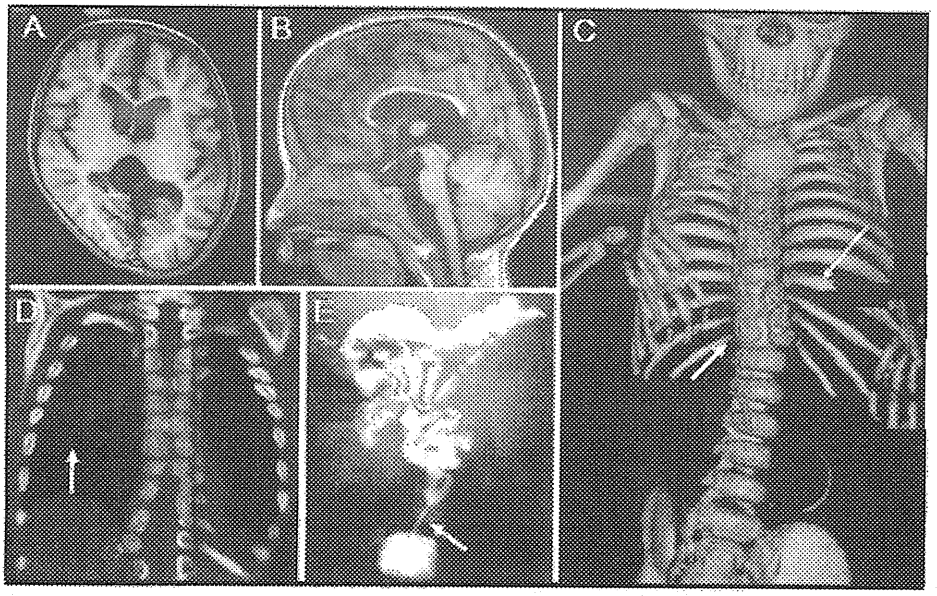


**FIG. 2. CT and MRI findings of the patient. A,B: Brain MRI (T1-weighted image) at 3 years of age showed decreased volume of the cortex in the frontal and parietal lobes, the presence of a subdural cyst in the corpora quadrigemina, and dilatation of the lateral and fourth ventricle. C: A bone survey performed using 3D CT showed abnormal segmentation of the ninth rib and an imbalanced hemivertebrae in the two lowest thoracic vertebral bodies (shown with arrows). D: CT of the chest showed CCAM (indicated by the arrow) in the right upper lobe. E: Barium enema showed a reduced caliber rectum (indicated by the arrow), suggesting that the patient had Hirschsprung disease.**

## Chromosomal and Molecular Genetic Studies

Genomic DNA isolated from the patient's peripheral white cells by phenol/chloroform extraction was used for *MBTPS2* mutation analysis. PCR-amplified DNA fragments were isolated using the QIAEX II Gel Extraction Kit (Qiagen, Valencia, CA) and purified using polyethylene glycol 6000 precipitation. PCR products were sequenced with the Big Dye Terminator Cycle Sequencing Kit V1.1 and analyzed with the ABI PRISM 310 Genetic Analyzer (Life Technologies, Carlsbad, CA). We also performed G-banded chromosome analysis at a resolution of 400–550 bands, genome-wide subtelomere fluorescence in situ hybridization (FISH) analysis, and array comparative genomic hybridization (array CGH) using Whole Human Genome Oligo Microarray Kits 244K (Agilent Technologies Inc., Palo Alto, CA) to identify genomic abnormalities.

## RESULTS

G-banded chromosome analysis and genome-wide subtelomere FISH analyses did not show chromosomal rearrangements in the patient. Array CGH analysis did not show copy number changes in the patient's genome with the exception of known copy-number variations (CNVs). Since some patients with IFAP syndrome have been reported to present with several clinical features of BRESEK/BRESHECK syndrome, including severe intellectual disability, vertebral and renal anomalies, and Hirschsprung disease, we conducted a comprehensive sequencing analysis of all exons and intron–exon boundaries of *MBTPS2*. This analysis identified a missense mutation (c.1286G>A, [p.Arg429His]) in exon 10, which was previously reported for IFAP syndrome (Fig. 3). The mutation was also found in one allele of the mother (I-2), indicating that the mutation was of maternal origin and that the mother was a heterozygous carrier (Fig. 3).

## DISCUSSION

In this report, we describe the fourth male patient with BRESHECK syndrome in whom we identified a missense mutation (c.1286G>A, [p.Arg429His]) in *MBTPS2*, which is the causal gene for IFAP syndrome. *MBTPS2* encodes a membrane-embedded zinc metalloprotease, termed site-2 protease (S2P). S2P cleaves and activates cytosolic fragments of sterol regulatory element binding proteins (SREBP1 and SREBP2) and a family of bZIP membrane-bound transcription factors of endoplasmic reticulum (ER) stress sensors (ATF6, OASIS), after a first luminal proteolytic cut by site-1 protease (S1P) within Golgi membranes [Sakai et al., 1996; Ye et al., 2000; Kondo et al., 2005; Asada et al., 2011]. The SREBPs control the expression of many genes involved in the biosynthesis and uptake of cholesterol, whereas ATF6 and OASIS induce many genes that clean up accumulated unfolded proteins in the ER. Dysregulated SREBP activation, impaired lipid metabolism, and accumulation of unfolded proteins in the ER caused by *MBTPS2* mutations could lead to disturbed differentiation of epidermal structures, resulting in the symptom triad of IFAP syndrome [Cursiefen et al., 1999; Traboulsi et al., 2004; Elias et al., 2008]. Oeffner et al. [2009] first identified five missense mutations in *MBTPS2* in patients with IFAP

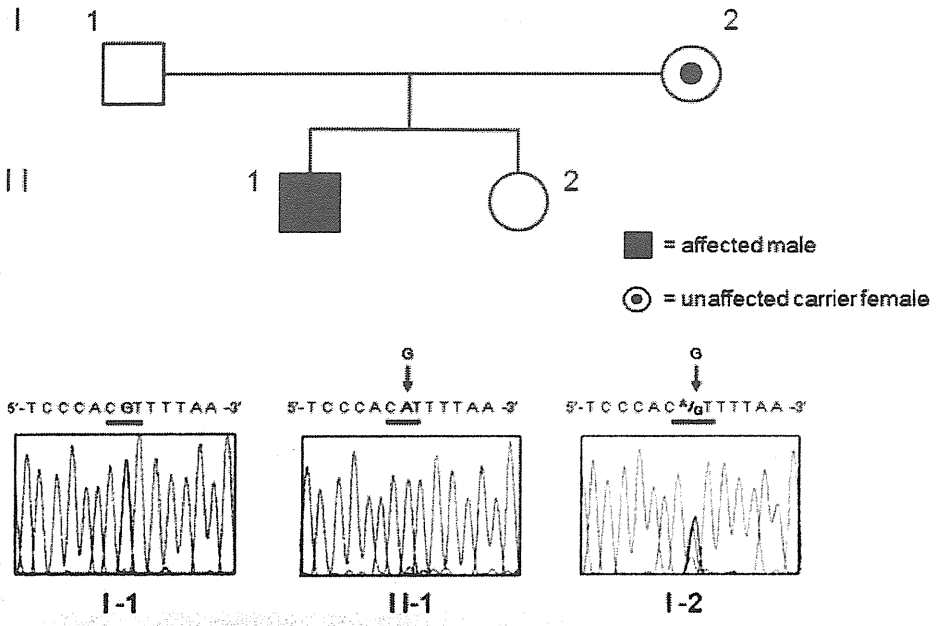


**FIG. 3. Identification of a disease mutation. The sequence analyses of the patient (II-1) showed a c.1286G>A variant in exon 10 of *MBTPS2*, which predicts p.Arg429His, as indicated by the arrow (middle panel). The mother (I-2) was heterozygous for the mutation ($C^A/_GT$) (right panel).**

syndrome. Transfection studies using wild type and mutant *MBTPS2* expression constructs demonstrated that the five *MBTPS2* mutations did not affect S2P protein amount and localization in the ER. However, enzyme activities, as measured by sterol responsiveness, were decreased in S2P-deficient M19 cells when the mutant *MBTPS2* was transiently expressed. Interfamilial phenotypic differences between male IFAP patients and the properties of mutants in functional assays predict a genotype–phenotype correlation, ranging from mild forms of the triad with relatively high enzyme activity (~80%) to severe manifestations of intellectual disability, various developmental defects, and early death with low enzyme activity (~15%). The identified p.Arg429His mutation in the patient reported here is one of the five missense mutations with the lowest enzyme activity. It was previously reported that all four patients harboring the p.Arg429His mutation died within 14 months of birth. The five mutations were not located in the HEIGH motif (amino acids [aa] 171–175) or in the $LD_{467}G$ sequence, both of which are regions important for coordinating the zinc atom at the enzymatic active site for protease activity in the Golgi membrane [Zelenski et al., 1999]. However, among the five mutations, the p.Arg429His mutation is located closest to the intramembranous domain, and it strongly reduced the enzymatic activity and caused a severe phenotype. This finding suggests that mutations in the HEIGH motif or in the $LD_{467}G$ sequence are fatal because they lead to a null function of the S2P. Although the detailed skin findings of the four patients with the p.Arg429His mutation have not been reported, it should be noted that one of the four patients (3-III:4) with the p.Arg429His mutation had brain anomaly, seizures, psychomotor retardation, vertebrae anomaly, Hirschsprung disease, absence of a kidney, atrial septum defect, and inguinal hernia, in addition to the symptom triad of IFAP syndrome [Oeffner et al., 2009]. These symptoms overlap with the majority of symptoms observed in BRESHECK syndrome (BRESHK; six of eight symptoms observed in BRESHECK) (Table I), and the present patient has BRESHECK syndrome. Collectively, these observations suggest that the most severe form of the syndrome caused by the p.Arg429His mutation in *MBTPS2* shows features quite similar or identical to those of BRESEK/BRESHECK syndrome.

There are two major differences in the definitions of IFAP syndrome and BRESEK/BRESHECK syndrome. Ichthyosis follicularis, one of the triad symptoms of IFAP syndrome, is a clinical condition of the skin. However, several studies on IFAP syndrome have reported various skin eruptions such as psoriasis-like and ichthyosis-like eruptions [Martino et al., 1992; Sato-Matsumura et al., 2000]. In contrast, patients with BRESEK/BRESHECK syndrome showed severe lamellar desquamation with diffuse scaling [Reish et al., 1997], similar to that observed in the present patient. This could be because of the difference in features of the skin, namely, ichthyosiform erythroderma-like appearance versus ichthyosis follicularis, in patients with the most severe forms of *MBTPS2* mutation and patients with IFAP syndrome who were described earlier, respectively.

The second difference is that photophobia was not described in the reported three male patients with BRESEK/BRESHECK syndrome [Reish et al., 1997; Tumialán and Mapstone, 2006]. In the present patient, photophobia became evident after he was diagnosed with BRESHECK syndrome. Photophobia is a symptom of epithelial disturbances of the cornea, such as ulceration and vascularization, which result in corneal scarring [Traboulsi et al., 2004]. In the most severe cases of *MBTPS2* mutation, such as

patients with severe intellectual disability who are bedridden and die early, it is likely that the patients were treated in the hospital without being exposed to sunlight. Therefore, it would be difficult to observe photophobia as a main symptom in those cases. Moreover, two previously described patients with BRESEK/BRESHECK syndrome had initial maldevelopment of one eye or small optic nerves. In these patients, photophobia may not have been obvious because of malformations of the eyes and optic nerves [Reish et al., 1997]. In our study, the patient showed clinical features of BRESHECK syndrome and photophobia with *MBTPS2* mutation, indicating that the clinical features of the present patient are extremely broad compared to the features of IFAP syndrome caused by *MBTPS2* mutation that have been previously reported [MacLeod, 1909].

Recently, a missense mutation (c.1523A>G, [p.Asn508Ser]) in *MBTPS2* was identified from 26 cases of three independent families with keratosis follicularis spinulosa decalvans (KFSD; OMIM# 308800), which is characterized by the development of hyperkeratotic follicular papules on the scalp followed by progressive alopecia of the scalp, eyelashes, and eyebrows in addition to childhood photophobia and corneal dystrophy [Aten et al., 2010]. A significant association was found between KFSD and the p.Asn508Ser mutation. The specific localization of alopecia to the scalp, eyelashes, and eyebrows and the limited childhood photophobia of KFSD indicate that KFSD has a relatively mild phenotype. The authors postulate that IFAP syndrome and KFSD are within the spectrum of one genetic disorder with a partially overlapping phenotype and propose that a new name should be chosen for KFSD/IFAP syndrome with an *MBTPS2* mutation. In contrast, the BRESHECK syndrome observed in the present patient has a severe phenotype caused by the p.Arg429His mutation. The present patient and the two patients (3-III:3 and 3-III:4) with the p.Arg429His mutation displayed broader clinical features, including eight features (BRESHECK) and six features (RESHCK and BRESHK) of BRESEK/BRESHECK syndrome, respectively (patients 4, 6, and 7; Table I) [Oeffner et al., 2009]. There is a debate regarding whether the two patients harboring six features were correctly diagnosed with BRESEK/BRESHECK syndrome since the patients did not have "BRESEK" but rather a combination of six other clinical features. To better understand and clearly distinguish the clinical features of the present patient from those of the reported patients with *MBTPS2* mutations, we propose the nomenclature of "BRESHECK/IFAP syndrome" for the present patient because he has clinical features of BRESHECK syndrome. We also suggest that the BRESHECK/IFAP syndrome be used for a broader definition that would include patients harboring most features of BRESHECK syndrome, including the previously reported two patients (3-III:3 and 3-III:4) with p.Arg429His mutation in *MBTPS2* [Oeffner et al., 2009]. Data from further genetic and clinical studies on more patients are required to determine which genes or *MBTPS2* mutations are associated with BRESEK/BRESHECK or BRESHECK/IFAP syndrome, respectively.

## ACKNOWLEDGMENTS

We thank the patient and his family for participating in the study. This study was supported by the Takeda Science Foundation (to N.W.) and by the Health Labour Sciences Research Grant (to S.M. and N.W.).

## REFERENCES

Aten E, Brasz LC, Bornholdt D, Hooijkaas IB, Porteous ME, Sybert VP, Vermeer MH, Vossen RH, van der Wielen MJ, Bakker E, Breuning MH, Grzeschik KH, Oosterwijk JC, den Dunnen JT. 2010. Keratosis follicularis spinulosa decalvans is caused by mutations in MBTPS2. Hum Mutat 31:1125–1133.

Asada R, Kanemoto S, Kondo S, Saito A, Imaizumi K. 2011. The signalling from endoplasmic reticulum-resident bZIP transcription factors involved in diverse cellular physiology. J Biochem 149:507–518.

Cursiefen C, Schlötzer-Schrehardt U, Holbach LM, Pfeiffer RA, Naumann GOH. 1999. Ocular findings in ichthyosis follicularis, atrichia, and photophobia syndrome. Arch Ophthalmol 117:681–684.

Elias PM, Williams ML, Holleran WM, Jiang YJ, Schmuth M. 2008. Pathogenesis of permeability barrier abnormalities in the ichthyoses: Inherited disorders of lipid metabolism. J Lipid Res 49:697–714.

Kondo S, Murakami T, Tatsumi K, Ogata M, Kanemoto S, Otori K, Iseki K, Wanaka A, Imaizumi K. 2005. OASIS, a CREB/ATF-family member, modulates UPR signalling in astrocytes. Nat Cell Biol 7:186–194.

MacLeod JMH. 1909. Three cases of 'ichthyosis follicularis' associated with baldness. Br J Dermatol 21:165–189.

Martino F, D'Eufemia P, Pergola MS, Finocchiaro R, Celli M, Giampà G, Frontali M, Giardini O. 1992. Child with manifestations of dermotrichic syndrome and ichthyosis follicularis alopecia photophobia (IFAP) syndrome. Am J Med Genet 44:233–236.

Oeffner F, Fischer G, Happle R, König A, Betz RC, Bornholdt D, Neidel U, Boente Mdel C, Redler S, Romero-Gomez J, Salhi A, Vera-Casaño A, Weirich C, Grzeschik KH. 2009. IFAP syndrome is caused by deficiency in MBTPS2, an intramembrane zinc metalloprotease essential for cholesterol homeostasis and ER stress response. Am J Hum Genet 84:459–467.

Reish O, Gorlin RJ, Hordinsky M, Rest EB, Burke B, Berry SA. 1997. Brain anomalies, retardation of mentality and growth, ectodermal dysplasia, skeletal malformations, Hirschsprung disease, ear deformity and deafness, eye hypoplasia, cleft palate, cryptorchidism, and kidney dysplasia/hypoplasia (BRESEK/BRESHECK): New X-linked syndrome? Am J Med Genet 68:386–390.

Sakai J, Duncan EA, Rawson RB, Hua X, Brown MS, Goldstein JL. 1996. Sterol-regulated release of SREBP-2 from cell membranes requires two sequential cleavages, one within a transmembrane segment. Cell 85: 1037–1046.

Sato-Matsumura KC, Matsumura T, Kumakiri M, Hosokawa K, Nakamura H, Kobayashi H, Ohkawara A. 2000. Ichthyosis follicularis with alopecia and photophobia in a mother and daughter. Br J Dermatol 142:157–162.

Traboulsi E, Waked N, Mégarbané H, Mégarbané A. 2004. Ocular findings in ichthyosis follicularis–alopecia–photophobia (IFAP) syndrome. Ophthal Genet 25:153–156.

Tumialán LM, Mapstone TB. 2006. A rare cause of benign ventriculomegaly with associated syringomyelia: BRESEK/BRESHECK syndrome. Case illustration. J Neurosurg 105:155.

Ye J, Rawson RB, Komuro R, Chen X, Davé UP, Prywes R, Brown MS, Goldstein JL. 2000. ER stress induces cleavage of membrane-bound ATF6 by the same proteases that process SREBPs. Mol Cell 6:1355–1364.

Zelenski NG, Rawson RB, Brown MS, Goldstein JL. 1999. Membrane topology of S2P, a protein required for intramembranous cleavage of sterol regulatory element-binding proteins. J Biol Chem 274:21973–21980.

# Progressive Atrophy of the Cerebrum in 2 Japanese Sisters with Microcephaly with Simplified Gyri and Enlarged Extraaxial Space

Authors

M. Hirose[1], K. Haginoya[1,2], H. Yokoyama[3], A. Kikuchi[1], N. Hino-Fukuyo[1], M. Munakata[1], M. Uematsu[1], K. Iinuma[4], M. Kato[5], T. Yamamoto[6], S. Tsuchiya[1]

Affiliations

Affiliation addresses are listed at the end of the article

Key words
- microcephaly
- simplified gyri
- enlarged extraaxial space
- atrophy

## Abstract

This is a case report that describes 2 sisters with microcephaly, simplified gyri, and enlarged extraaxial space. Clinical features of the cases include dysmorphic features, congenital microcephaly, failure of postnatal brain growth, neonatal onset of seizures, quadriplegia, and severe psychomotor delay. Neuroradiological imaging demonstrated hypoplasia of bilateral cerebral hemispheres with enlarged extraaxial spaces, simplified gyral patterns without a thickened cortex, hypoplastic corpus callosum, and enlarged lateral ventricles, with a reduction in gray and white matter volume during the prenatal and neonatal periods. Repeat MRI revealed progressive atrophy of the cerebral gray and white matter, with enlarged lateral ventricles, although the sizes of the bilateral basal ganglia, thalamus, and infratentorial structures were relatively preserved. These neuroradiological findings imply that this disease is caused by the gene involved in neuronal and glial proliferation in the ventricular zone and in tangential neuronal migration from the ganglionic eminence. The nature of the progressive degeneration of the hemispheric structures should be clarified.

received 25.04.2011
accepted 28.08.2011

Bibliography
DOI http://dx.doi.org/10.1055/s-0031-1287771
Neuropediatrics 2011; 42: 163–166

ISSN 0174-304X

Correspondence
*Kazuhiro Haginoya, MD, PhD*
Department of Pediatric Neurology
Takuto Rehabilitation Center for Children
20 Shikaoto
Akiu Yumoto
Taihaku-ku
Sendai 982-0241
Japan
Tel.: +81/22/398 2221
Fax: +81/22/397 2697
khaginoya@silk.ocn.ne.jp

## Introduction

From medical records and brain images in 237 patients with brain malformations characterized as microcephaly with simplified gyri, Basel-Vanagaite and Dobyns classified patients into 4 major groups: microcephaly with simplified gyri only, microcephaly with simplified gyri and pontocerebeller hypoplasia, microcephaly with simplified gyri and enlarged extraaxial space, and microcephaly with simplified gyri and both pontocerebeller hypoplasia and enlarged extraaxial space [1]. One of these groups, microcephaly with simplified gyri and enlarged extraaxial space is clinically characterized by severe developmental failure, feeding difficulty, spastic quadriplegia, and dyskinesia, with postnatal or congenital brain growth failure [occipital frontal circumference (OFC) below − 3 SD]. MRI findings typically show microcephaly, simplified gyri, enlarged extraaxial space and relatively preserved pontocerebeller structures [1]. In this case study, we describe 2 Japanese sisters with microcephaly with simplified gyri and enlarged extraaxial space. In one of the sisters, repeat MRI findings showed progressive atrophy of the cerebral hemispheres.

## Case Report

### Patient 1

The older sister, the first child of unrelated parents, was born after 38 weeks gestation by spontaneous delivery following a normal pregnancy. Microcephaly was noted during fetal ultrasonographic examination in the last trimester. The patient's birth weight was 2400 g (−1.5 SD), length 45.0 cm (−1.7 SD), and OFC 30 cm (−2.2 SD). She temporally showed clonic seizure activity on day 0. Upon admission at the age of 1 month, her general condition was unremarkable in spite of microcephaly and feeding difficulties. Dysmorphic features including a sloping forehead, arched and thick eyebrows, blephalophimosis, a saddle nose, triangular mouth, and micrognathia were observed. She began having complex partial seizures with right facial clonic seizures at 2 months of age. The seizures were controlled with valproic acid. The patient had spastic quadriplegia without obvious spontaneous movements and gastroesophageal reflux disease (GERD) beginning at 3 months of age. She died suddenly at 4 years and 8 months of age.

Laboratory examinations were normal including blood $NH_3$, blood gas analysis, serum lactate, blood glucose, cerebrospinal fluid (CSF) glucose, CSF lactate, CSF white cell count, blood amino acid analysis, urine organic acid analysis, and plasma very long-chain fatty acid (VLCFA). Chromosome analysis and fluorescent in situ hybridization (FISH) studies for the LIS1 specific deletion at 17p13.3 revealed no abnormalities.

Her electroencephalogram (EEG) showed low amplitude and irregular waking background without obvious epileptic discharges on day 0. The ictal EEG of complex partial seizures at 3 months of age revealed right fronto-central spike bursts. Auditory evoked potentials (ABRs) and visual evoked potentials (VEPs) both showed a flat pattern. Brain magnetic resonance imaging (MRI) on day 0 revealed hypoplasia of bilateral cerebral hemispheres with enlarged extraaxial space, a simplified gyral pattern without a thickened cortex, a relatively spared volume of the bilateral basal ganglia and thalamus, a mildly flattened brain stem, and a hypoplastic corpus callosum (◎ **Fig. 1a–c**).

### Patient 2

The microcephaly of the younger sister was recognized at a gestational age (GA) of 28 weeks by means of ultrasonography. She was born after 37 weeks gestation by spontaneous delivery following a normal pregnancy. The patient's birth weight was 2566 g (−0.5 SD), length 46.0 cm (−0.7 SD), and OFC 27 cm (−4.0 SD). Her Apgar score was 8 at 1 min, and 9 at 5 min. She developed generalized tonic seizures at 3 months of age. Her seizures were well controlled with valproic acid beginning when she was 2 years old.

She was able to bottle feed through the first 12 months, but her feeding skills deteriorated beginning at 18 months of age. At 2 years and 6 months, she was also diagnosed with GERD and required the use of a duodenal feeding tube. She also had spastic quadriplegia and visual impairment from early infancy. No developmental progress was observed.

Clinical examination performed at 3 years and 1 month of age showed microcephaly of OFC 41.5 cm (−4.2 SD), and other growth parameters were between −1 and −2 SD. Her dysmorphism was similar to that of her older sister. She had marked scoliosis, with hypertonic extremities and a posture characterized by asymmetrical tonic neck reflex. Deep tendon reflexes were exaggerated, and ankle clonus appeared bilaterally. Erratic myoclonus in the bilateral orbicular muscles and systemic myoclonus easily induced by sounds were often seen. There was no spontaneous movement of the extremities.

Laboratory examinations were normal including blood chemistry, creatinine kinase, intrauterine infection screen, blood $NH_3$, blood gas analysis, serum lactate, serum glucose, CSF glucose, CSF lactate, CSF white cell count, blood amino acid analysis, urine organic acid analysis, and plasma VLCFA. Chromosome analysis (G band) was 46XX; FISH for the LIS1 specific deletion at 17p13.3 was negative. Array-based comparative genomic hybridization (array-CGH) was performed using the Agilent Human Genome Microarray kit 244A (Agilent Technologies, Santa Clara, CA, USA), and it showed no apparent deletions or duplication.

The brain MRIs were performed at a GA of 30 weeks via intrauterine imaging, at day 0, and at 3 years and 1 month (◎ **Fig. 2a–g**). The former 2 MRI findings were almost identical to those of the older sister. Cerebellar white matter around the dentate nucleus had high $T_2$ signal intensity, showing unmyelinated cerebellar white matter. The MRI at 3 years and 1 month of age demonstrated marked dilatation of the posterior and inferior horns of the lateral ventricles and severe volume reduction of whole hemispheric gray and white matter, which was most dominant in the frontal lobes, whereas the volumes of bilateral basal ganglia, thalamus, and infratentorial structures were relatively preserved. The patient's EEG at 4 months of age and 3 years and 1 month of age demonstrated almost continuous spikes in the mid-frontal to right frontal regions. ABR and VEP were normal.

## Discussion

There have been only 3 reports describing patients with microcephaly with simplified gyri and enlarged extraaxial space [1, 2, 8]. None of these reports included repeat MRI studies. As in the previous reports, our patients suggested an autosomal recessive trait of inheritance. Alternatively, an autosomal dominant or X-linked dominant inheritance with gonadal mosaisism is also possible. The genes responsible for microcephaly with simplified gyri only have been identified as *MCPH1, ASPM, CDK5RAP2, CENPJ,* and *WDR62* [1, 9]. However, it is not clear whether microcephaly with simplified gyri and enlarged extraaxial space with this phenotypic presentation can be explained by different mutation patterns of the already identified genes or whether it represents a distinct disease entity caused by still unknown genes. The extraaxial space enlargement described previously was less severe as compared to the present cases [1]. Dysmorphic features as observed in the present patients have not been described previously, although multiple anomalies, eye defects and jejunal atresia have been reported in patients with microcephaly with simplified gyri [1]. It remains to be clarified whether those phenotypic and neuroradiological features suggest distinctive clinical entity. Moreover, there may be overlap in the MRI findings between patients with microcephaly with simplified gyri and enlarged extraaxial space and those with microcephaly with simplified gyri and both enlarged extraaxial space

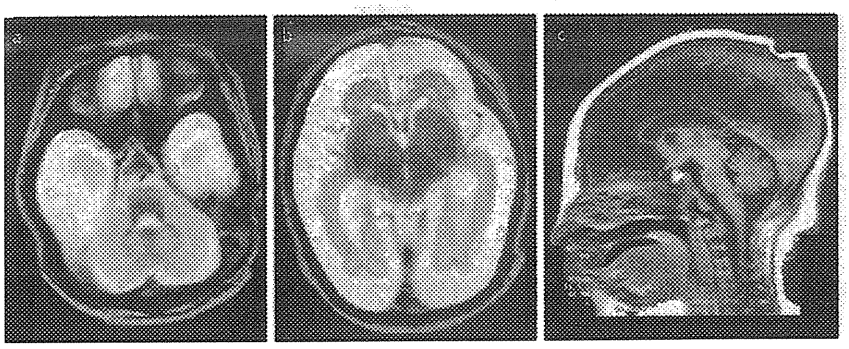

**Fig. 1** Brain MRI of older sister at age of day 0. The MRI (**a** and **b**: $T_2$-weighted image [TR 4000, TE 132], **c**: $T_1$-weighted image [TR 500, TE 14.0]) showing hypoplasia of bilateral cerebral hemispheres with enlarged extraaxial space, a simplified gyral pattern without a thickened cortex, hypoplastic corpus callosum, and a mildly flattened brain stem.

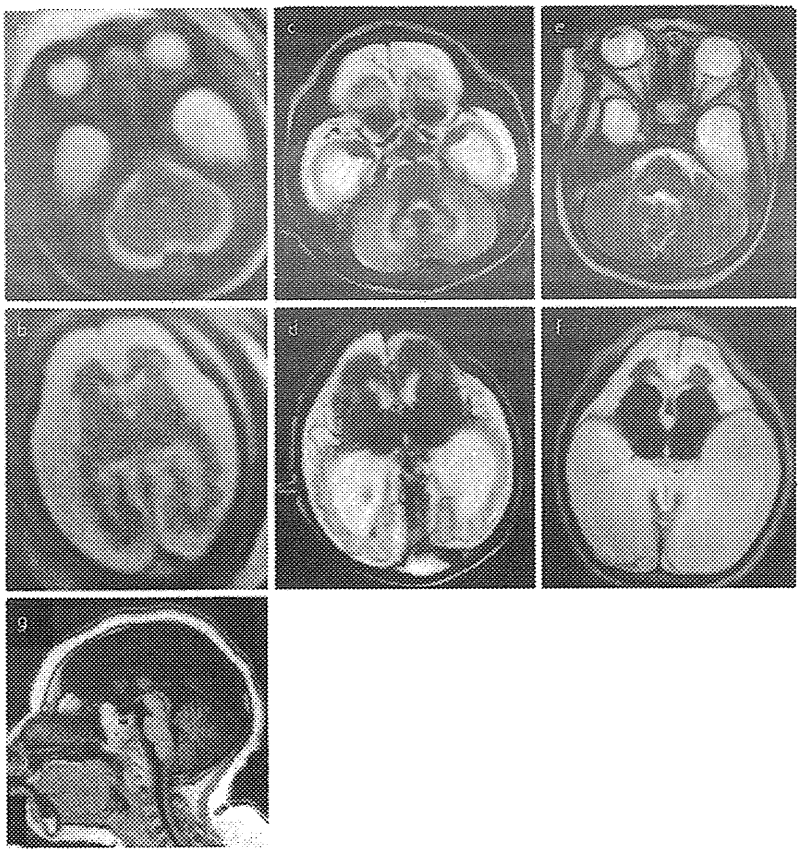

**Fig. 2** Brain MRI with $T_2$-weighted images [TR 4500, TE 90] (**a–f**) and $T_1$-weighted images [TR 500, TE 14.0] (**g**) of the younger sister at 30 weeks gestational age (**a**, **b**), day 0 (**c**, **d**), and 3 years and 1 month of age (**e–g**). The MRI at 30 weeks gestational age and day 0 (**a–d**) revealed hypoplasia of bilateral cerebral hemispheres, particularly in the frontal regions, with enlarged extraaxial space, a simplified gyral pattern without thickened cortex, and enlarged lateral ventricles, especially in the posterior and temporal horns, with a reduction in the surrounding white matter. There was no change in the findings between GA 30 weeks and day 0. High signal intensity was observed in the lateral sides of the dentate nucleus (**c**). The MRI at 3 years and 1 month of age (**e–g**) demonstrated progressive dilatation of the posterior and inferior horns of the lateral ventricles, with a volume reduction in the surrounding hemispheric structures, especially in the frontal lobe. Some extent of myelination in the cerebellar hemisphere was observed (**e**). The size of the basal ganglia and thalamus, as well as of the infratentorial structures, was relatively preserved (**g**).

and pontocerebeller hypoplasia, because the older sister in our study had a mildly flattened brain stem at age of day 0. On the other hand, pontocerebeller hypoplasia may be the result of extensive cerebral pathology, as seen in the pontocerebeller hypoplasia in preterm infants [7].

A striking finding in these patients was progressive atrophy of the cerebral gray and white matter, with enlarged lateral ventricles, which was evident in the younger sister. Neurodegenerative processes such as accelerated apoptosis may be estimated from the MRI findings described in this report and the clinical deterioration observed in the younger sister. Basel-Vanagaite and Dobyns also described a rapid decrease in OFC postnatally in the subgroup of patients without congenital microcephaly but with enlarged extraaxial space [1]. Similar progressive changes in the cerebrum have also been reported in a patient most likely categorized as microcephaly with simplified gyri and pontocerebeller hypoplasia [4].

In spite of remarkable volume reductions in cerebral hemisphere cortices and white matter, the size of the bilateral basal ganglia, thalamus, and infratentorial structures was relatively preserved in these cases. As a cortical ribbon was formed and periventricular nodular heterotopia or band heterotopia was not observed, migration of cortical neurons from the ventricular zone may not be involved, but the proliferation process of neuronal and glial cells in the ventricular zone may be altered. On the other hand, the proliferation of neuronal cells in the lateral ganglionic eminence that generates the striatum and in the medial ganglionic eminence that mostly generates the globus pallidus and septum [3,6] may not be involved, although tangential migration of cortical GABAergic interneurons from the ganglionic eminence may have been altered [5].

In conclusion, it is believed that the genes responsible for microcephaly with simplified gyri and enlarged extraaxial space are involved in the neuronal and glial proliferation in the ventricular zone as well as in tangiential neuronal migration. Moreover, the nature of progressive degeneration of the hemispheric structures should be clarified in the near future.

Affiliations

[1]Department of Pediatrics, Tohoku University School of Medicine, Sendai, Japan
[2]Department of Pediatric Neurology, Takuto Rehabilitation Center for Children, Sendai, Japan
[3]Department of Nursing, Yamagata University Faculty of Medicine, Yamagata, Japan
[4]Ishinomaki Red Cross Hospital, Ishinomaki, Japan
[5]Department of Pediatrics, Yamagata University Faculty of Medicine, Yamagata, Japan
[6]Tokyo Women's Medical University Institute for Integrated Medical Sciences, Tokyo, Japan

## References

1 *Basel-Vanagaite L, Dobyns WB.* Clinical and brain imaging heterogeneity of severe microcephaly. Pediatr Neurol 2010; 43: 7–16
2 *Basel-Vanagaite L, Marcus N, Klinger G et al.* New syndrome of simplified gyral pattern, micromelia, dysmorphic features and early death. Am J Med Genet A 2003; 119: 200–206
3 *Deacon TW, Pakzaban P, Isacson O.* The lateral ganglionic eminence is the origin of cells committed to striatal phenotypes: neural transplantation and developmental evidence. Brain Res 1994; 668: 211–219
4 *Kure-Kageyama H, Saito Y, Maegaki Y et al.* A patient with simplified gyral pattern followed by progressive brain atrophy. Brain Dev 2007; 29: 383–386
5 *Letinic K, Zoncu R, Rakic P.* Origin of GABAergic neurons in the human neocortex. Nature 2002; 417: 645–649

6 *Olsson M, Campbell K, Wictorin K et al.* Projection neurons in fetal striatal transplants are predominantly derived from the lateral ganglionic eminence. Neuroscience 1995; 69: 1169–1182
7 *Srinivasan L, Allsop J, Counsell SJ et al.* Smaller cerebellar volumes in very preterm infants at term-equivalent age are associated with the presence of supratentorial lesions. AJNR Am J Neuroradiol 2006; 27: 573–579
8 *Woods CG, Bond J, Enard W.* Autosomal recessive primary microcephaly (MCPH): a review of clinical, molecular, and evolutionary findings. Am J Hum Genet 2005; 76: 717–728
9 *Yu TW, Mochida GH, Tischfield DJ et al.* Mutations in WDR62, encoding a centrosome-associated protein, cause microcephaly with simplified gyri and abnormal cortical architecture. Nat Genet 2010; 42: 1015–1020

CLINICAL REPORT

AMERICAN JOURNAL OF medical genetics

# Dandy–Walker Malformation Associated With Heterozygous *ZIC1* and *ZIC4* Deletion: Report of a New Patient

**Jun Tohyama,[1,2]* Mitsuhiro Kato,[3] Sari Kawasaki,[4] Naoki Harada,[5] Hiroki Kawara,[5] Takeshi Matsui,[5] Noriyuki Akasaka,[1] Tsukasa Ohashi,[1] Yu Kobayashi,[1] and Naomichi Matsumoto[6]**

[1]Department of Pediatrics, Nishi-Niigata Chuo National Hospital, Niigata, Japan

[2]Department of Pediatrics, Niigata University Medical and Dental Hospital, Niigata, Japan

[3]Department of Pediatrics, Yamagata University School of Medicine, Yamagata, Japan

[4]Department of Neurology, Saigata National Hospital, Jouetsu, Japan

[5]Department of Molecular Genetic Testing, Clinical Laboratory Center, Mitsubishi Chemical Medience Corporation, Nagasaki, Japan

[6]Department of Human Genetics, Yokohama City University Graduate School of Medicine, Yokohama, Japan

Received 10 February 2010; Accepted 9 July 2010

We report on a female patient with Dandy–Walker malformation possibly caused by heterozygous loss of *ZIC1* and *ZIC4*. The patient presented with mental retardation, epilepsy, and multiple congenital malformations including spina bifida, mild dysmorphic facial features including, thick eyebrows, broad nose, full lips, macroglossia, and hypoplasia of the cerebellar vermis with enlargement of the fourth ventricle on brain magnetic resonance imaging, which is consistent with Dandy–Walker malformation. A chromosome analysis showed interstitial deletion of chromosome 3q23-q25.1. Fluorescence in situ hybridization (FISH) and microarray-based genomic analysis revealed the heterozygous deletion of *ZIC1* and *ZIC4* loci on 3q24. Her facial features were not consistent with those observed in blepharophimosis–ptosis–epicanthus inversus syndrome (BPES) involving *FOXL2* abnormality. Other deleted genes at 3q23-25.1 might contribute to the dysmorphic facial appearance. A milder phenotype as the Dandy–Walker malformation in our patient supports the idea that modifying loci/genes can influence the development of cerebellar malformation. 

**Key words:** Dandy–Walker malformation; interstitial deletion 3q; *ZIC1*; *ZIC4*

How to Cite this Article:
Tohyama J, Kato M, Kawasaki S, Harada N, Kawara H, Matsui T, Akasaka N, Ohashi T, Kobayashi Y, Matsumoto N. 2011. Dandy–Walker malformation associated with heterozygous *ZIC1* and *ZIC4* deletion: Report of a new patient.
Am J Med Genet Part A 155:130–133.

## INTRODUCTION

Dandy–Walker malformation (DWM) is an abnormality in the development of the central nervous system that is defined by hypoplasia and upward rotation of the cerebellar vermis and cystic dilatation of the fourth ventricle [Hart et al., 1972; Parisi and Dobyns, 2003]. DWM is etiologically heterogeneous in association with a wide variety of chromosomal anomalies, various Mendelian disorders, multifactorial disorders, and environmental factors [Murray et al., 1985; Chitayat et al., 1994].

Grinberg et al. [2004] described seven nonrelated patients of DWM with de novo interstitial deletions of chromosome 3q. Cytogenetic investigation of these patients showed the first critical region involved in DWM, which encompasses genes *ZIC1* and *ZIC4*. There are five *Zic* genes encoding zinc finger proteins in humans and mice [Grinberg and Millen, 2005]. *ZIC1* and *ZIC4* are tightly linked on human chromosome 3 and mouse chromosome 9 [Grinberg et al., 2004; Grinberg and Millen, 2005]. A heterozygous deletion of these two linked genes in mice resulted in a phenotype that closely resembles DWM [Grinberg et al., 2004], strongly suggesting that heterozygous deletion of both *ZIC1* and *ZIC4* is the cause of DWM in humans. This is the second report on a new patient of DWM with heterozygous *ZIC1* and *ZIC4* deletion.

Grant sponsor: Ministry of Health, Labor and Welfare; Grant number: 20A-14.

*Correspondence to:
Jun Tohyama, M.D., Department of Pediatrics, Nishi-Niigata Chuo National Hospital, 1-14-1 Masago, Nishi-ku, Niigata 950-2085, Japan.
E-mail: jtohyama@masa.go.jp

Published online 10 December 2010 in Wiley Online Library (wileyonlinelibrary.com).
DOI 10.1002/ajmg.a.33652

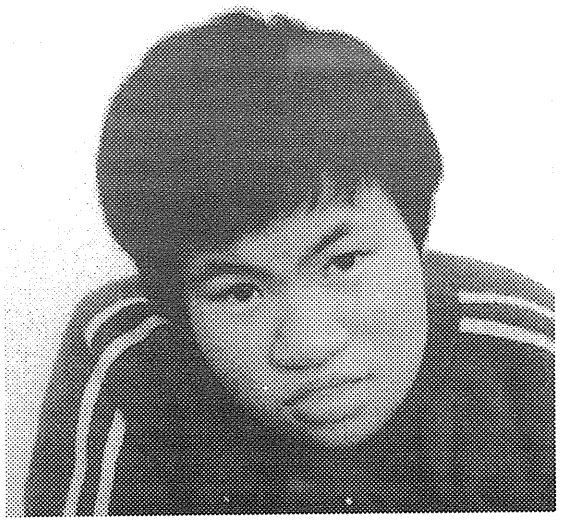

**FIG. 1. Photograph of our patient at 21 years of age. Thick eyebrows, broad nose, and full lips are notable.**

## CLINICAL REPORT

A girl, the third child of healthy nonconsanguineous parents, was born at 41 weeks gestation by normal vaginal delivery following an uneventful pregnancy. Her elder brother has had epilepsy since age 10, however, his mental development was normal. Her birth weight was 2,880 g, length was 48 cm, and occipitofrontal circumference was 33 cm. A sacral dimple associated with occult spine bifida was found at birth. Computed tomography (CT) of the brain showed no sign of hydrocephalus. Follow-up CT at the age of 3 years showed mild dilatation of lateral ventricles. No treatment including surgical intervention was required at that time. Dislocation of both hip joints was also noted. After delivery, the patient received tube feeding for 3 months because of feeding difficulties and poor body weight gain. Her development was severely delayed: she could crawl by herself at age 1 year, and walk alone at 8 years. Hip joint dislocation was surgically repaired at 3 years. At 11 years, she developed generalized seizures, which were uncontrollable by various anti-epileptic drugs. On admission at 11 years, she showed dysmorphic features including thick eyebrows, a broad nose, full lips, and macroglossia, but no blepharophimosis/ptosis (Fig. 1). Mild scoliosis was also noted. Neurological examination revealed she had left hemiparesis with contracture of the lower and upper limbs. Both lower limbs were atrophic. Myoclonic movements on the left limbs were observed. Signs of cranial nerve impairment or cerebellar ataxia were evident. Electroencephalography identified a right-sided delta activity in the frontal lobe. Radiogram of facial bone showed no abnormal findings. Magnetic resonance imaging (MRI) of the brain showed hypoplasia and upward rotation of the cerebellar vermis and enlargement of the fourth ventricle, indicating DWM (Fig. 2A,B). The lateral ventricles were also enlarged. At 19 years, she could not speak. She could not walk alone because of deteriorating left hemiparesis with frequent seizures. She showed regular menstruation after menarche at 15 years.

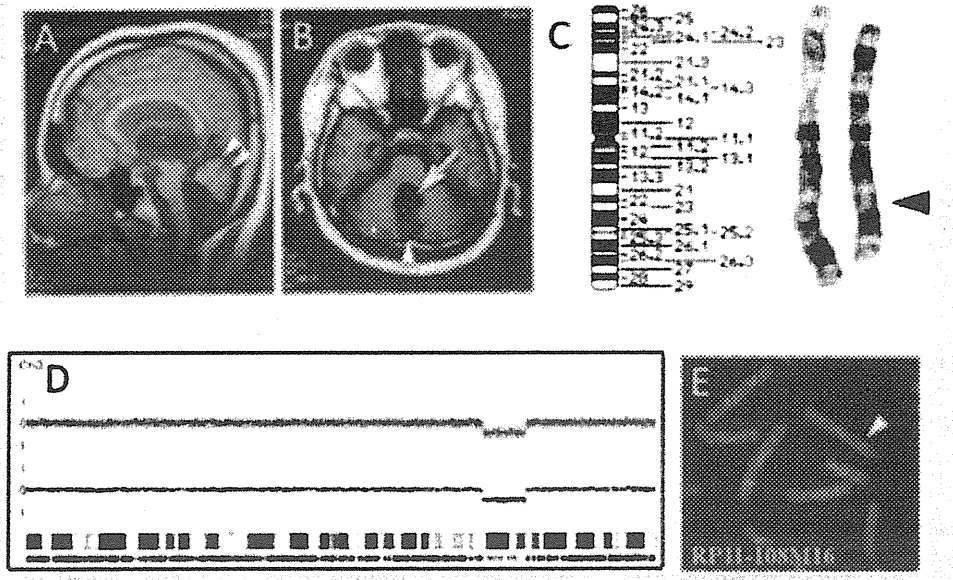


**FIG. 2. A: Brain magnetic resonance imaging of the patient. Midline sagittal T1-weighted image shows hypoplasia and upward rotation of the cerebellar vermis (white arrowheads). B: Brain magnetic resonance imaging of the patient. Transverse T1-weighted image shows hypoplasia of the cerebellar hemisphere and vermis, and enlarged the fourth ventricle (white arrow). The fourth ventricle communicates with the posterior fossa fluid space (white arrowhead). C: Partial karyotype of the patient: del(3)(q23q25.1). The arrowhead indicates deletion. D: SNP chip analysis. A 14-Mb deletion is clearly demonstrated using CNAG 2.0 software. E: FISH analysis. RP11-108M16 covering *ZIC1* and *ZIC4* shows a heterozygous deletion (white arrowhead).**

### Cytogenetic and Genomic Analysis

Chromosomal analysis of her peripheral blood lymphocytes revealed that her karyotype was 46,XX,del(3)(q23q25.1) (Fig. 2C). Normal karyotype was confirmed in her parents. Her elder brother was not examined because abnormal features were not observed. To define chromosome 3q deletion, we performed genomic copy number analysis by GeneChip 250K Nsp Array (Affymetrix, Santa Clara, CA) and CNAG 2.0 software [Nannya et al., 2005] using the DNA of the patient's peripheral blood leukocytes. Copy number analysis clearly demonstrated the 14-Mb interstitial deletion: arr 3q23q25.31 (142,479,100–156,504,521) × 1 (Fig. 2D). According to the UCSC Genome Browser Human February 2009 Assembly, the deletion contains 67 RefSeq genes including following OMIM genes, *ATR*, *PLOD2*, *ZIC4*, *ZIC1*, *AGTR1*, *HPS3*, *CP*, *CLRN1*, *P2RY12*, and *MME*. Fluorescence in situ hybridization (FISH) using three BAC clones, RP11-108M16 (covering *ZIC4* and *ZIC1*), RP11-1001A3, and RP11-71N10 at 3q24, confirmed the deletion (Fig. 2E).

## DISCUSSION

This patient presented with multiple congenital malformations, including occult spina bifida, dysmorphic facial features, and hypoplasia, and upward rotation of the cerebellar vermis with enlargement of the fourth ventricle on brain MRI, which were consistent with DWM. A cytogenetic analysis showed interstitial deletion of chromosome 3q23 to 3q25.1, and her FISH study confirmed the heterozygous deletion of *ZIC1* and *ZIC4* on 3q24. Recently, Grinberg et al. [2004] reported that locus 3q24 is the first critical region involved in DWM, encompassing genes *ZIC1* and *ZIC4*. The human ZIC gene family encoding zinc-finger transcription factors is comprised of five members [Grinberg and Millen, 2005]. The ZIC gene family is expressed in central nervous systems, including the cerebellum, and *Zic* genes are found to be expressed in the adult mouse cerebellum in a highly restricted manner [Aruga et al., 1994, 1996, 2002]. *Zic1* plays essential roles in cerebellar development, and the *Zic1* gene deletion could cause the extracerebellar phenotype as those reported in the *Zic1* knockout mice [Aruga et al., 1998; Ogura et al., 2001]. Human *ZIC1* and *ZIC4* are both mapped to 3p24. A mouse model for only $Zic1^{+/-}$ or $Zic4^{+/-}$ showed a slightly hypoplastic cerebellum, however, 15% of these double heterozygotes have severe cerebellar hypoplasia [Grinberg et al., 2004]. The authors conclude that heterozygous loss of *ZIC1* and *ZIC4* is the cause of DWM in individuals with deletion of 3q2. In our patient, we also demonstrated the heterozygous deletion of both *ZIC1* and *ZIC4* by FISH and SNP array. After the original report of seven cases, this is the second report dealing with the eighth case of DWM with heterozygous *ZIC1* and *ZIC4* deletion.

The original seven patients showed various phenotypes such as DWM. A wide variety of deletion in size was noted. The cerebellar hypoplasia in our patient is moderately severe as compared with those in the original seven cases. Chromosomal deletion in our patient ranges from 3q23 to 3q25.1. Grinberg et al. [2004] stated that the severity of DWM does not correlate with the size of chromosomal deletion. In the $Zic1^{+/-}$ $Zic4^{+/-}$ mice, 85% had a mild cerebellar phenotype whereas 15% were severely affected. The authors speculated that the variable expressivity observed in humans and mice might support the idea of modifying loci influencing the development of cerebellar malformation.

Three of the seven individuals in the report of Grinberg et al. [2004] have facial changes observed in the blepharophimosis–ptosis–epicanthus inversus syndrome (BPES), representing a recognizable contiguous gene syndrome [Smith et al., 1989; Ishikiriyama and Goto, 1993]. BPES is also an autosomal dominant inheritance and maps to 3q23 [Amati et al., 1995]. Crisponi et al. [2001] identified the forkhead transcription factor gene 2 (*FOXL2*) gene as responsible for BPES, which is located 3q22.3-q23. The facial dysmorphology of our patient is not consistent with BPES. To define her deletion, we performed a SNP array-based genomic copy number analysis and found that her interstitial deletion did not involve *FOXL2*. Only one of the five patients with 3q23-q25 deletion in the earlier reports showed no clinical features resembling BPES [Franceschini et al., 1983; Alvarado et al., 1987]. Dysmorphic facial features of this patient included synophrys of the eyebrows, broad nose, and full lips [Franceschini et al., 1983], partially resembling those of our case. Other deleted genes may affect the dysmorphic facial features in our patient.

DWM is a relatively common malformation of the central nervous system, but this condition has etiologic heterogeneity. After finding the first critical region of DWM, DeScipio et al. [2005] identified six children with subtelomeric deletions of 6p25, which is the second locus of DWM, and Aldinger et al. [2009] reported that the alteration of *FOXC1* at 6p25.3 contributed to DWM. In addition, Jalali et al. [2008] reported on a male patient with a heterozygous deletion of distal 2q, and identified a candidate locus for DWM with occipital cephalocele at 2q36.1 by linkage analysis. Their family showed an autosomal dominant mode of inheritance.

The recurrence risk for DWM is also heterogeneous, depending on the etiology, which is not yet fully explained despite intensive cytogenetic investigations of many cases. Empiric recurrence risk for DWM in the absence of a known disorder is relatively low [Murray et al., 1985]. High-resolution chromosomal analysis of patients may provide critical information necessary for genetic counseling related to DWM.

## ACKNOWLEDGMENTS

The authors thank Dr. Masashi Suda and Dr. Shigeru Maruyama for providing patient information. This study was supported in part by a Research Grant (20A-14) for Nervous and Mental Disorders from the Ministry of Health, Labor and Welfare.

## REFERENCES

Aldinger KA, Lehmann OJ, Hudgins L, Chizhikov VV, Bassuk AG, Ades LC, Krantz ID, Dobyns WB, Millen KJ. 2009. *FOXC1* is required for normal cerebellar development and is a major contributor to chromosome 6p25.3 Dandy–Walker malformation. Nat Genet 41:1037–1042.

Alvarado M, Bocian M, Walker AP. 1987. Interstitial deletion of the long arm of chromosome 3: Case report, review, and definition of a phenotype. Am J Med Genet 27:781–786.

Amati P, Chomel JC, Nivelon-Chevalier A, Gilgenkrantz S, Kitzis A, Kaplan J, Bonneau D. 1995. A gene for blepharophimosis-ptosis-epicanthus inversus syndrome maps to chromosome 3q23. Hum Genet 96:213–215.

Aruga J, Yokota N, Hashimoto M, Furuichi T, Fukuda M, Mikoshiba K. 1994. A novel zinc finger protein, Zic, is involved in neurogenesis, especially in the cell lineage of cerebellar granule cells. J Neurochem 63:1880–1890.

Aruga J, Nagai T, Tokuyama T, Hayashizaki Y, Okazaki Y, Chapman VM, Mikoshiba K. 1996. The mouse *Zic* gene family. Homologues of the *Drosophila* pair-rule gene *odd-paired*. J Biol Chem 271:1043–1047.

Aruga J, Minowa O, Yaginuma H, Kuno J, Nagai T, Noda T, Mikoshiba K. 1998. Mouse *Zic1* is involved in cerebellar development. J Neurosci 18:284–293.

Aruga J, Tohmonda T, Homma S, Mikoshiba K. 2002. Zic1 promotes the expansion of dorsal neural progenitors in spinal cord by inhibiting neuronal differentiation. Dev Biol 244:329–341.

Chitayat D, Moore L, Del Bigio MR, MacGregor D, Ben-Zeev B, Hodgkinson K, Deck J, Stothers T, Ritchie S, Toi A. 1994. Familial Dandy–Walker malformation associated with macrocephaly, facial anomalies, developmental delay, and brain stem dysgenesis: Prenatal diagnosis and postnatal outcome in brothers. A new syndrome? Am J Med Genet 52:406–415.

Crisponi L, Deiana M, Loi A, Chiappe F, Uda M, Amati P, Bisceglia L, Zelante L, Nagaraja R, Porcu S, Ristaldi MS, Marzella R, Rocchi M, Nicolino M, Lienhardt-Roussie A, Nivelon A, Verloes A, Schlessinger D, Gasparini P, Bonneau D, Cao A, Pilia G. 2001. The putative forkhead transcription factor *FOXL2* is mutated in blepharophimosis/ptosis/epicanthus inversus syndrome. Nat Genet 27:159–166.

DeScipio C, Schneider L, Young TL, Wasserman N, Yaeger D, Lu F, Wheeler PG, Williams MS, Bason L, Jukofsky L, Menon A, Geschwindt R, Chudley AE, Saraiva J, Schinzel AAGL, Guichet A, Dobyns WE, Toutain A, Spinner NB, Krantz ID. 2005. Subtelomeric deletions of chromosome 6p: Molecular and cytogenetic characterization of three new cases with phenotypic overlap with Ritscher-Shinzel (3C) syndrome. Am J Med Genet Part A 134A:3–11.

Franceschini P, Silengo MC, Davi G, Bianco R, Biagioli M. 1983. Interstitial deletion of the long arm of chromosome 3 in a patient with mental retardation and congenital anomalies. Hum Genet 64:97.

Grinberg I, Millen KJ. 2005. The *ZIC* gene family in development and disease. Clin Genet 67:290–296.

Grinberg I, Northrup H, Ardinger H, Prasad C, Dobyns WB, Millen KJ. 2004. Heterozygous deletion of the linked genes *ZIC1* and *ZIC 4* is involved in Dandy–Walker malformation. Nat Genet 36: 1053–1055.

Hart MN, Malamud N, Ellis WG. 1972. The Dandy–Walker syndrome. A clinicopathological study based on 28 cases. Neurology 22:771–780.

Ishikiriyama S, Goto M. 1993. Blepharophimosis sequence (BPES) and microcephaly in a girl with del(3)(q22.2q23): A putative gene responsible for microcephaly close to the BPES gene? Am J Med Genet 47: 487–489.

Jalali A, Aldinger KA, Chary A, Mclone DG, Bowman RM, Le LC, Jardine P, Newbury-Ecob R, Mallick A, Jafari N, Russell EJ, Curran J, Nguyen P, Ouahchi K, Lee C, Dobyns WB, Millen KJ, Pina-Neto JM, Kessler JA, Bassuk AG. 2008. Linkage to chromosome 2q36.1 in autosomal dominant Dandy–Walker malformation with occipital cephalocele and evidence for genetic heterogeneity. Hum Genet 123:237–245.

Murray JC, Johnson JA, Bird TD. 1985. Dandy–Walker malformation: etiologic heterogeneity and empiric recurrence risks. Clin Genet 28: 272–283.

Nannya Y, Sanada M, Nakazaki K, Hosoya N, Wang L, Hangaishi A, Kurokawa M, Chiba S, Bailey DK, Kennedy GC, Ogawa S. 2005. A robust algorithm for copy number detection using high-density oligonucleotide single nucleotide polymorphism genotyping arrays. Cancer Res 65: 6071–6079.

Ogura H, Aruga J, Mikoshiba K. 2001. Behavioral abnormalities of *Zic1* and *Zic2* mutant mice: implications as models for human neurological disorders. Behav Genet 31:317–324.

Parisi MA, Dobyns WB. 2003. Human malformations of the midbrain and hindbrain: review and proposed classification scheme. Mol Genet Metab 80:36–53.

Smith A, Fraser IS, Shearman RP, Russell P. 1989. Blepharophimosis plus ovarian failure: a likely candidate for a contiguous gene syndrome. J Med Genet 26:434–438.

OPEN ACCESS Freely available online

PLoS one

# Two Novel Mutations in the *EYS* Gene Are Possible Major Causes of Autosomal Recessive Retinitis Pigmentosa in the Japanese Population

**Katsuhiro Hosono[1]*, Chie Ishigami[2], Masayo Takahashi[2], Dong Ho Park[3], Yasuhiko Hirami[4], Hiroshi Nakanishi[5], Shinji Ueno[6], Tadashi Yokoi[7], Akiko Hikoya[1], Taichi Fujita[1], Yang Zhao[1,8], Sachiko Nishina[7], Jae Pil Shin[3], In Taek Kim[3], Shuichi Yamamoto[9], Noriyuki Azuma[7], Hiroko Terasaki[6], Miho Sato[1], Mineo Kondo[6], Shinsei Minoshima[8], Yoshihiro Hotta[1]**

**1** Department of Ophthalmology, Hamamatsu University School of Medicine, Hamamatsu, Japan, **2** Laboratory for Retinal Regeneration, RIKEN Center for Developmental Biology, Kobe, Japan, **3** Department of Ophthalmology, Kyungpook National University Hospital, Daegu, Korea, **4** Department of Ophthalmology, Institute of Biomedical Research and Innovation Hospital, Kobe, Japan, **5** Department of Otolaryngology, Hamamatsu University School of Medicine, Hamamatsu, Japan, **6** Department of Ophthalmology, Nagoya University Graduate School of Medicine, Nagoya, Japan, **7** Department of Ophthalmology and Laboratory of Cell Biology, National Center for Child Health and Development, Tokyo, Japan, **8** Department of Photomedical Genomics, Basic Medical Photonics Laboratory, Medical Photonics Research Center, Hamamatsu University School of Medicine, Hamamatsu, Japan, **9** Department of Ophthalmology and Visual Science, Chiba University Graduate School of Medicine, Chiba, Japan

## Abstract

Retinitis pigmentosa (RP) is a highly heterogeneous genetic disease including autosomal recessive (ar), autosomal dominant (ad), and X-linked inheritance. Recently, arRP has been associated with mutations in *EYS* (Eyes shut homolog), which is a major causative gene for this disease. This study was conducted to determine the spectrum and frequency of *EYS* mutations in 100 Japanese arRP patients. To determine the prevalence of *EYS* mutations, all *EYS* exons were screened for mutations by polymerase chain reaction amplification, and sequence analysis was performed. We detected 67 sequence alterations in *EYS*, of which 21 were novel. Of these, 7 were very likely pathogenic mutations, 6 were possible pathogenic mutations, and 54 were predicted non-pathogenic sequence alterations. The minimum observed prevalence of distinct *EYS* mutations in our study was 18% (18/100, comprising 9 patients with 2 very likely pathogenic mutations and the remaining 9 with only one such mutation). Among these mutations, 2 novel truncating mutations, c.4957_4958insA (p.S1653KfsX2) and c.8868C>A (p.Y2956X), were identified in 16 patients and accounted for 57.1% (20/35 alleles) of the mutated alleles. Although these 2 truncating mutations were not detected in Japanese patients with adRP or Leber's congenital amaurosis, we detected them in Korean arRP patients. Similar to Japanese arRP results, the c.4957_4958insA mutation was more frequently detected than the c.8868C>A mutation. The 18% estimated prevalence of very likely pathogenic mutations in our study suggests a major involvement of *EYS* in the pathogenesis of arRP in the Japanese population. Mutation spectrum of *EYS* in 100 Japanese patients, including 13 distinct very likely and possible pathogenic mutations, was largely different from the previously reported spectrum in patients from non-Asian populations. Screening for c.4957_4958insA and c.8868C>A mutations in the *EYS* gene may therefore be very effective for the genetic testing and counseling of RP patients in Japan.

**Citation:** Hosono K, Ishigami C, Takahashi M, Park DH, Hirami Y, et al. (2012) Two Novel Mutations in the *EYS* Gene Are Possible Major Causes of Autosomal Recessive Retinitis Pigmentosa in the Japanese Population. PLoS ONE 7(2): e31036. doi:10.1371/journal.pone.0031036

**Editor:** Michael Edward Zwick, Emory University School Of Medicine, United States of America

**Received** September 9, 2011; **Accepted** December 30, 2011; **Published** February 17, 2012



**Funding:** This study was supported by research grants from the Ministry of Health, Labour and Welfare (Research on Measures for Intractable Diseases) and from the Japan Society for the Promotion of Science (Grant-in-Aid for Scientific Research (C) 23592561 and Grant-in Aid for Young Scientists (B) 23791975). The funders had no role in study design, data collection and analysis, decision to publish, or preparation of the manuscript.

**Competing Interests:** The authors have declared that no competing interests exist.

* E-mail: hosono@hama-med.ac.jp

## Introduction

Retinitis pigmentosa (RP [MIM 268000]) is a highly heterogeneous genetic disease characterized by night blindness and visual field constriction leading to severe visual impairment. The disease appears with different modes of inheritance including autosomal recessive (ar), autosomal dominant (ad), and X-linked, and currently over half of cases are isolated in Japan.

To date, 53 causative genes and 7 loci of RP have been identified (http://www.sph.uth.tmc.edu/Retnet/), including the eyes shut homolog (*EYS*) gene encoding an ortholog of *Drosophila* spacemaker (spam), a protein essential for photoreceptor morphology. *EYS* spans over 2 Mb, making it one of the largest known genes expressed in the human eye [1,2]. *EYS* gene mutations, primarily truncating and some missense mutations, have been detected in arRP families of different ancestral origin and have reported to account for 5–16% of arRP [3–6]. Most gene mutations (e.g., *RHO*, *PRPH2*, *PRPF31*, *RP1*, and *IMPDH1*) have been found in Japanese patients with adRP, with few reports describing mutations in arRP [7,8]. Therefore, the genes causing arRP in most Japanese families have yet to be identified.

In this study, we screened all *EYS* gene exons in 100 unrelated Japanese RP patients. We found 2 novel truncating *EYS* gene mutations that were surprisingly related to 16% of Japanese arRP patients, but were not detected in Japanese patients with either adRP or Leber's congenital amaurosis (LCA [MIM204000], the earliest onset and most severe form of hereditary retinal dystrophy with several clinical features overlapping with those of RP). Additionally, these mutations were also detected in 9% of Korean arRP patients.

## Methods

### Patients and clinical evaluation

We screened all *EYS* gene exons in 100 unrelated Japanese RP patients with no systemic manifestations, excluding families with obvious autosomal dominant inheritance. Some pedigrees showed a pattern compatible with the recessive mode of inheritance; the other patients were considered isolated cases. In addition, 200 unrelated and non-RP Japanese individuals were screened as controls to evaluate the frequency of the mutations found in the patient samples. We also screened a part of *EYS* gene exons 26 and 44 in 19 unrelated Japanese adRP patients, 28 unrelated Japanese LCA patients, and 32 unrelated Korean arRP patients. The 19 Japanese adRP patients had already been screened for some principal adRP-causing genes, but the pathogenic mutations have not yet been detected. Examples of the screening list for adRP-causing genes and targeted exons include exon 3 and 4 in *RP1*; exon 1, 2, 3, 4, and 5 in *RHO*; exon 1, 2, and 3 in *PRPH2*; exon 2, 3, and 4 in *CRX*; exon 11 in *PRPF3*; exon 10, 11, and 12 in *IMPDH1*; exon 2 in *NRL*; exon 43 in *PRPF8*; exon 1 and 2 in *ROM1*; exon 5 and 6 in *RP9*; exon 2, 3, 5, 6, 7, 8, 11, and 12 in *PRPF31*; exon 11 and 15 in *SEMA4A*; exon 1 in *CA4*; exon 3 in *GUCA1B*; exon 3 in *SP4*; and exon 3 in *TOPORS*.

Japanese RP patients were examined either at the Department of Ophthalmology, Hamamatsu University Hospital in Hamamatsu (by YH), Department of Ophthalmology, Kobe City Medical Center General Hospital in Kobe (by MT), or Department of Ophthalmology, Nagoya University Hospital in Nagoya (by MK). Patients' origin varied widely, from the Tokyo to Osaka areas in Japan. Japanese LCA patients were examined at the Department of Ophthalmology and Laboratory of Cell Biology, National Center for Child Health and Development in Tokyo (by NA). LCA patients' origin varied widely, from all over Japan except the Okinawa islands. Meanwhile, Korean RP patients were examined at the Department of Ophthalmology, Kyungpook National University Hospital in Daegu (by ITK). The Korean patients' origin varied widely, from Daegu to Yeongju and Pohang areas in Gyeongsangbuk-do, Korea. A full ophthalmic examination was performed. Clinical diagnosis for RP was based on visual field, fundus examination, and electroretinogram findings, and clinical diagnosis for LCA was based on fundus examination and electroretinogram findings.

### Ethics statements

This study was approved by the Institutional Review Board for Human Genetic and Genome Research at the 6 participating institutions (Hamamatsu University School of Medicine, RIKEN Center for Developmental Biology, Nagoya University Graduate School of Medicine, National Center for Child Health and Development, Chiba University Graduate School of Medicine, and Kyungpook National University Hospital), and its procedures conformed to the tenets of the Declaration of Helsinki. Written informed consent was obtained from all participants before molecular genetic studies.

### Mutation analysis

Genomic DNA in Japanese samples was extracted from the peripheral lymphocytes using standard procedures. In Korean samples, whole blood samples were collected on FTA cards (GE Healthcare). Blood samples were spotted onto the cards and air-dried for 1 h at room temperature. For polymerase chain reaction (PCR) amplification, a 1.2-mm disk was punched from a dried blood spot using a Harris micro-punch tool (GE Healthcare) and processed according to the manufacturer's instructions. PCR was performed using the KOD -Plus- ver. 2 PCR kit (Toyobo) with the primer sets described in Table S1 for 35 cycles of 98°C for 10 s, 60°C for 30 s, and 68°C for 1 min in an automated thermal cycler (GeneAmp PCR System 9700; Applied Biosystems). PCR products were purified with Wizard SV Gel and PCR Clean-up System (Promega) or treated with Exonuclease I and Antarctic Phosphatase (New England Biolabs). Direct sequencing was performed using the BigDye Terminator v3.1 Cycle Sequencing Kit on an ABI3100 autosequencer (Applied Biosystems). For Japanese arRP patients, all 44 exons, including 3 non-coding exons (exons 1–3) that cover the 5′ untranslated region and 41 coding exons (exons 4–44), were analyzed in both sense and antisense directions. For Japanese adRP and LCA patients, and Korean arRP patients, parts of exons 26 and 44 were analyzed (Table S1).

### Assessment of pathogenicity

A sequence variant was considered pathogenic if it represented a truncating mutation (nonsense or frameshift), large-scale deletion mutation, or missense mutation affecting a conserved amino acid residue and did not appear in control samples (number of alleles studied ≤400) and/or in a public SNP database (http://www.ncbi.nlm.nih.gov/projects/SNP/). Particularly, missense mutations were considered pathogenic if found together with a second variant, especially if it was truncating. As reference data, we employed 4 computational algorithms to evaluate the pathogenicity of missense mutations: SIFT (http://sift.jcvi.org/www/SIFT_seq_submit2.html), PolyPhen2 (http://genetics.bwh.harvard.edu/pph2/), PMut (http://mmb.pcb.ub.es/PMut/), and SNAP (http://rostlab.org/services/snap/).

## Results

### Mutation analysis

Mutation analysis of *EYS* in 100 unrelated Japanese patients revealed 7 very likely pathogenic mutations in 18 patients (18%). Of these 18 patients, a second mutant allele could not be detected in 9 patients. The very likely pathogenic mutations consisted of 3 truncating mutations, 1 deletion mutation, 2 missense mutations, and 1 previously described mutation (Fig. 1, Table 1, and Table 2). In addition, we also identified 6 possible pathogenic mutations in 8 separate patients (Table 1 and Table 2).

A novel truncating insertion, c.4957_4958insA, was detected in 12 patients and accounted for 15 of the 35 mutated alleles detected (42.9%) (Table 1 and Table 2). Three patients were homozygous for the c.4957_4958insA mutation, and the other 9 patients were heterozygous. Of the latter, 3 patients showed the second mutation while 6 did not. This insertion creates a frameshift mutation that predicts a premature stop at codon 1654 (p.S1653KfsX2). A novel truncating nonsense mutation c.8868C>A (p.Y2956X) was identified in 4 patients and accounted for 5 of the 35 mutated alleles detected (14.3%). Thus, these 2 novel truncating mutations were identified in 16 separate patients, resulting in a very high frequency of the 2 mutations in Japanese arRP patients.

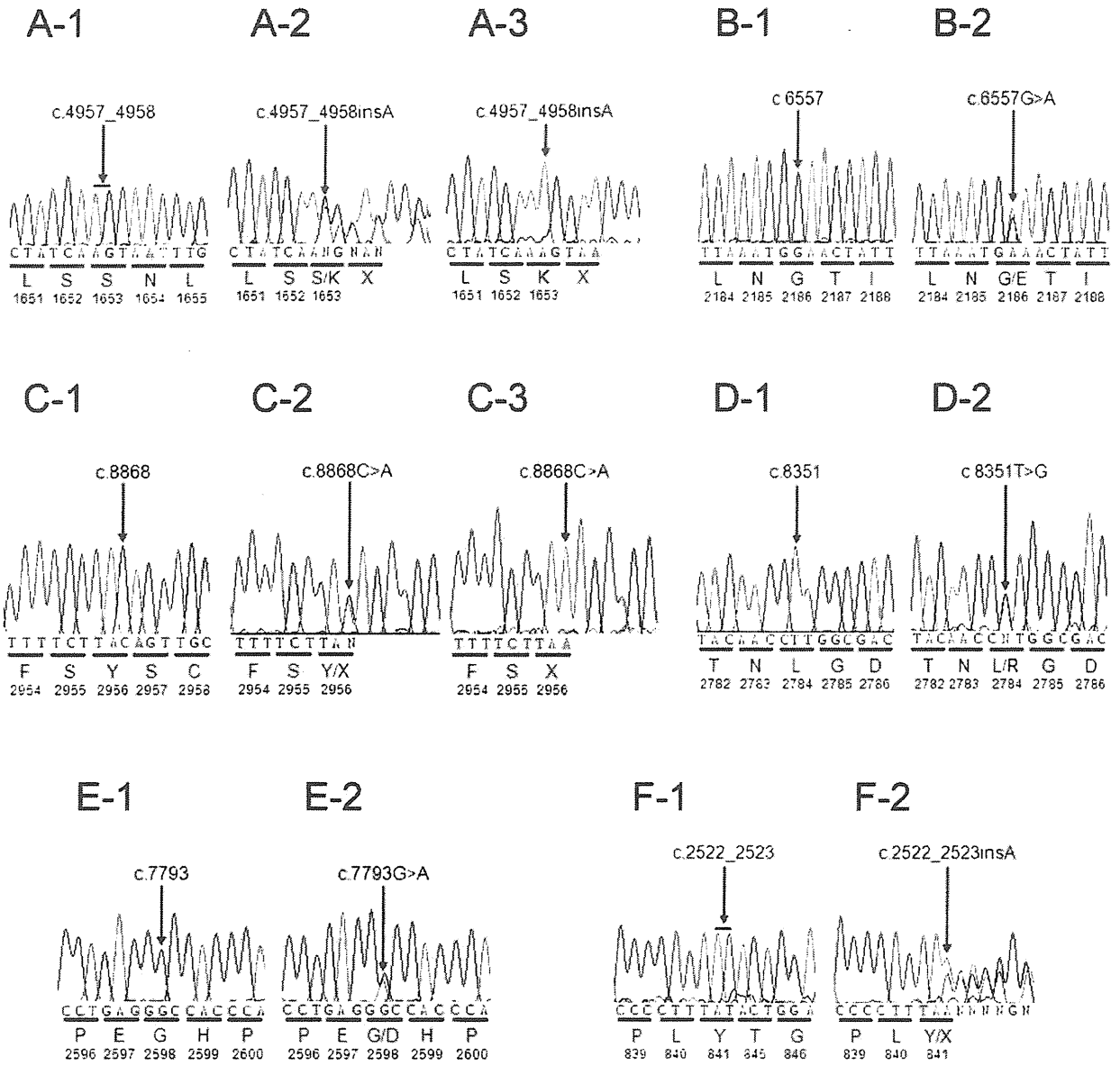


**Figure 1. Electropherograms of the 6 likely pathogenic *EYS* mutations.** Partial sequence of the *EYS* gene showing the normal control sequences (A-1 through F-1), heterozygous mutation sequences (A-2 through F-2), and homozygous mutation sequences (A-3 and C-3). Deduced amino acids are indicated under the sequence trace. The mutation location is indicated either by an arrow (for a nucleotide change) or a horizontal line (to show 2 nucleotides between which the insertion occurred). (A) c.4957_4958insA; p.S1653KfsX2 (Exon 26), (B) c.6557G>A; p.G2186E (Exon 32), (C) c.8868C>A; p.Y2956X (Exon 44), (D) c.8351T>G; p.L2784R (Exon 44), (E) c.7793G>A; p.G2598D (Exon 40), (F) c.2522_2523insA; p.Y841X (Exon 16). doi:10.1371/journal.pone.0031036.g001

## Families with very likely pathogenic mutations and both alleles affected

Nine of the 18 patients bearing very likely pathogenic mutations appeared to have both alleles affected, suggesting that they received one mutated allele from each unaffected parent (Table 1 and Table 2). In 4 patients (RP3H, RP48K, RP56K, and RP81K), segregation analysis was performed, and the 2 pathogenic alleles were considered to be on different chromosomes (Fig. 2).

1. In RP3H, proband (II-6) was homozygous for c.4957_4958insA. The mutation co-segregated with the phenotype: the unaffected brother (II-4) demonstrated wild-type alleles, while the affected brother (II-5) was homozygous for the mutation.
2. In RP48K, proband (II-1) was homozygous for c.4957_4958insA. The unaffected brother (II-2) was heterozygous for the mutation.
3. In RP56K, proband (II-1) was compound heterozygous for c.4957_4958insA and missense mutation c.8351T>G (p.L2784R). The mutation co-segregated with the phenotype: the affected brother (II-2) also showed both mutations, while the unaffected brother (II-3) was heterozygous for c.4957_4958insA.

**Table 1.** Mutation spectrum of the *EYS* gene in Japanese families.

| Family ID | Nucleotide change | Predicted effect | Domain[a] | Location in gene | Type of change | Reference |
|---|---|---|---|---|---|---|
| **Families with very likely pathogenic mutations and both alleles affected** | | | | | | |
| RP3H[b] | c.4957_4958insA/ c.4957_4958insA | p.S1653KfsX2/ p.S1653KfsX2 | Close to coiled-coil/ Close to coiled-coil | Exon 26/Exon 26 | Homozygous | This study |
| **RP48K[b]** | **c.4957_4958insA/ c.4957_4958insA** | **p.S1653KfsX2/ p.S1653KfsX2** | **Close to coiled-coil/ Close to coiled-coil** | **Exon 26/Exon 26** | **Homozygous** | **This study** |
| RP54K | c.4957_4958insA/ c.4957_4958insA | p.S1653KfsX2/ p.S1653KfsX2 | Close to coiled-coil/ Close to coiled-coil | Exon 26/Exon 26 | Homozygous | This study |
| **RP44K** | **c.4957_4958insA/ c.6557G>A** | **p.S1653KfsX2/ p.G2186E** | **Close to coiled-coil/ Laminin G** | **Exon 26/Exon 32** | **Heterozygous/ Heterozygous** | **This study/Abd El-Aziz et al., 2010; Littink et al., 2010; This study** |
| RP56K[b] | c.4957_4958insA/ c.8351T>G | p.S1653KfsX2/ p.L2784R | Close to coiled-coil/ Laminin G | Exon 26/Exon 44 | Compound Heterozygous | This study |
| **RP87N** | **c.4957_4958insA/ c.7793G>A** | **p.S1653KfsX2/ p.G2598D** | **Close to coiled-coil/ Close to Laminin G** | **Exon 26/Exon 40** | **Heterozygous/ Heterozygous** | **This study** |
| RP81K[b] | c.2522_2523insA/ c.6557G>A | p.Y841X/p.G2186E | EGF/Laminin G | Exon 16/Exon 32 | Compound Heterozygous | This study/Abd El-Aziz et al., 2010; Littink et al., 2010; This study |
| **RP21H** | **deletion exon32/ deletion exon32** | **p.D2142_S2191delinsG/ p.D2142_S2191delinsG** | **Laminin G/Laminin G** | **Exon 32/Exon 32** | **Homozygous** | **This study** |
| RP35K | c.8868C>A/c.8868C>A | p.Y2956X/p.Y2956X | EGF/EGF | Exon 44/Exon 44 | Homozygous | This study |
| **Families with single very likely pathogenic mutations** | | | | | | |
| RP1H | c.4957_4958insA | p.S1653KfsX2 | Close to coiled-coil | Exon 26 | Heterozygous | This study |
| **RP6H** | **c.4957_4958insA** | **p.S1653KfsX2** | **Close to coiled-coil** | **Exon 26** | **Heterozygous** | **This study** |
| RP12H | c.4957_4958insA | p.S1653KfsX2 | Close to coiled-coil | Exon 26 | Heterozygous | This study |
| **RP51K** | **c.4957_4958insA** | **p.S1653KfsX2** | **Close to coiled-coil** | **Exon 26** | **Heterozygous** | **This study** |
| RP96H | c.4957_4958insA | p.S1653KfsX2 | Close to coiled-coil | Exon 26 | Heterozygous | This study |
| **RP100N** | **c.4957_4958insA** | **p.S1653KfsX2** | **Close to coiled-coil** | **Exon 26** | **Heterozygous** | **This study** |
| RP8H | c.8868C>A | p.Y2956X | EGF | Exon 44 | Heterozygous | This study |
| **RP25H** | **c.8868C>A** | **p.Y2956X** | **EGF** | **Exon 44** | **Heterozygous** | **This study** |
| RP80K[b] | c.8868C>A | p.Y2956X | EGF | Exon 44 | Heterozygous | This study |
| **Families with single possible pathogenic mutations** | | | | | | |
| RP4H | c.9272T>C | p.I3091T | Laminin G | Exon 44 | Heterozygous | This study |
| **RP9H** | **c.8875C>A** | **p.L2959M** | **EGF** | **Exon 44** | **Heterozygous** | **This study** |
| RP49K | c.9272T>C | p.I3091T | Laminin G | Exon 44 | Heterozygous | This study |
| **RP53K** | **c.5884A>G** | **p.T1962A** | **Laminin G** | **Exon 28** | **Heterozygous** | **This study** |
| RP55K | c.9272T>C | p.I3091T | Laminin G | Exon 44 | Heterozygous | This study |
| **RP74K** | **c.5404C>T** | **p.L1802F** | **Close to Laminin G** | **Exon 26** | **Heterozygous** | **This study** |
| RP79K | c.77G>A | p.R26Q | Close to signal peptide cleavage site | Exon 4 | Heterozygous | This study |
| **RP83K** | **c.2923T>C** | **p.C975R** | **EGF** | **Exon 19** | **Heterozygous** | **This study** |

Nucleotide numbering reflects cDNA numbering with +1 corresponding to the A of the ATG translation initiation codon in the reference sequence FM209056, according to the nomenclature recommended by the Human Genome Variation Society (www.hgvs.org/mutnomen). The initiation codon is codon 1. None of these 13 mutations were found in the Japanese controls.

[a]EYS has a signal peptide, a putative coiled-coil, 29 EGF, and 5 Laminin G domains. See Fig. 3.

[b]Segregation analysis has been performed. See Fig. 2.

In RP56K and RP81K, 2 pathogenic alleles were considered to be on different chromosomes (compound heterozygous). See Fig. 2.

doi:10.1371/journal.pone.0031036.t001

4. In RP81K, proband (II-5) was compound heterozygous for truncating insertion c.2522_2523insA (p.Y841X) and missense mutation c.6557G>A (p.G2186E). This insertion results in premature termination of the encoded protein at codon 841 (p.Y841X). Missense mutation c.6557G>A has been previously reported as disease causing in one Korean/American and one Chinese patient [3,6]. The unaffected mother (I-2) was heterozygous for c.2522_2523insA, while the unaffected sister (II-6) was heterozygous for c.6557G>A.

For the other patients, segregation analysis could not be performed due to difficulties in collecting samples from the families of patients (Table 1). RP54K and RP35K were homozygous for truncating mutation c.4957_4958insA and c.8868C>A, respectively. RP21H was homozygous for deletion in exon 32, an in-frame deletion that results in the replacement of amino acids from D2142 to S2191 with G2142 (p.D2142_S2191delinsG) and disrupts the second laminin G domain (Fig. 3). RP44K and RP87N were heterozygous for truncating and missense mutations, c.4957_4958insA/c.6657G>A (p.G2186E) and